

BASIC SCIENCES

Nobiletin Prevents High-Fat Diet-Induced Dysregulation of Intestinal Lipid Metabolism and Attenuates Postprandial Lipemia

Nadya M. Morrow, Natasha A. Trzaskalski¹, Antonio A. Hanson¹, Evgenia Fadzeyeva, Dawn E. Telford¹, Sanjiv S. Chhoker, Brian G. Sutherland, Jane Y. Edwards, Murray W. Huff¹, Erin E. Mulvihill¹

OBJECTIVE: Nobiletin is a dietary flavonoid that improves insulin resistance and atherosclerosis in mice with metabolic dysfunction. Dysregulation of intestinal lipoprotein metabolism contributes to atherogenesis. The objective of the study was to determine if nobiletin targets the intestine to improve metabolic dysregulation in both male and female mice.

APPROACH AND RESULTS: Triglyceride-rich lipoprotein (TRL) secretion, intracellular triglyceride kinetics, and intestinal morphology were determined in male and female LDL (low-density lipoprotein) receptor knockout (*Ldlr*^{-/-}), and male wild-type mice fed a standard laboratory diet or high-fat, high-cholesterol (HFHC) diet \pm nobiletin using an olive oil gavage, radiotracers, and electron microscopy. Nobiletin attenuated postprandial TRL levels in plasma and enhanced TRL clearance. Nobiletin reduced fasting jejunal triglyceride accumulation through accelerated TRL secretion and lower jejunal fatty acid synthesis with no impact on fatty acid oxidation. Fasting-refeeding experiments revealed that nobiletin led to higher levels of phosphorylated AKT (protein kinase B) and FoxO1 (forkhead box O1) and normal Srebp1c expression indicating increased insulin sensitivity. Intestinal length and weight were diminished by HFHC feeding and restored by nobiletin. Both fasting and postprandial plasma GLP-1 (glucagon-like peptide-1; and likely GLP-2) were elevated in response to nobiletin. Treatment with a GLP-2 receptor antagonist, GLP-2(3-33), reduced villus length in HFHC-fed mice but did not impact TRL secretion in any diet group. In contrast to males, nobiletin did not improve postprandial lipid parameters in female mice.

CONCLUSIONS: Nobiletin opposed the effects of the HFHC diet by normalizing intestinal de novo lipogenesis through improved insulin sensitivity. Nobiletin prevents postprandial lipemia because the enhanced TRL clearance more than compensates for increased TRL secretion.

GRAPHIC ABSTRACT: A [graphic abstract](#) is available for this article.

Key Words: apolipoprotein B-48 ■ glucagon-like peptides ■ insulin resistance ■ lipoproteins ■ triglycerides

Central to the metabolic syndrome is insulin resistance, which drives the predominance of small, dense LDL (low-density lipoprotein) particles, the reduction of HDL (high-density lipoprotein)-cholesterol, and increased fasting and postprandial concentrations of apoB (apolipoprotein-B)-containing TRL.¹ In the setting of diabetes, where dyslipidemia is exacerbated, statin therapy achieves target LDL-cholesterol levels. Still, it does not eliminate cardiovascular risk.^{1–3} Analysis from the REDUCE-IT (Reduction of Cardiovascular Events with Icosapent Ethyl-Intervention Trial) has demonstrated

that patients on statins with elevated triglyceride levels can further reduce their cardiovascular risk through targeting triglyceride concentrations.⁴

Intestinal enterocytes absorb and package dietary lipids for storage in cytoplasmic lipid droplets (CLDs) or into chylomicrons.⁵ It is increasingly appreciated that intestinal lipid handling and lipoprotein synthesis are regulated by dietary lipid supply, hormonal signaling,⁶ and circulating fatty acids (FA).^{7,8} In wild-type (WT) mice, acute insulin injection following an olive oil gavage reduced plasma triglyceride through increased phosphorylation of

Correspondence to: Erin E. Mulvihill, University of Ottawa Heart Institute, Room 3229A, 40 Ruskin Rd, Ottawa, ON K1Y4W7. Email emulvihi@uottawa.ca
Supplemental Material is available at <https://www.ahajournals.org/doi/suppl/10.1161/ATVBAHA.121.316896>.

For Sources of Funding and Disclosures, see page 143.

© 2021 American Heart Association, Inc.

Arterioscler Thromb Vasc Biol is available at www.ahajournals.org/journal/atvb

Nonstandard Abbreviations and Acronyms

CLDs	cytoplasmic lipid droplets
FA	fatty acid
FoxO1	forkhead box O1
GLP-1	glucagon-like peptide-1
HDL	high-density lipoprotein
HFHC	high-fat, high-cholesterol
LDL	low-density lipoprotein
LDLR	LDL receptor
LPL	lipoprotein lipase
LTT	lipid tolerance test
mTORC1	mammalian target of rapamycin complex 1
MTP	microsomal triglyceride transfer protein
NEFA	nonesterified FA
REDUCE-IT	Reduction of Cardiovascular Events with Icosapent Ethyl-Intervention Trial
SLD	standard laboratory diet
SREBP-1c	sterol regulatory element binding protein 1c
TRL	triglyceride-rich lipoprotein
VLDL	very-low-density lipoprotein
WT	wild type

intestinal AKT (protein kinase B), reduced MTP (microsomal triglyceride transfer protein) expression and activity.⁹ Chronic high-fat feeding induces changes in intestinal nutrient metabolism; however, it is debated whether they result from adaptation or obesity-induced dysregulation.^{10–13} In WT mice, these changes include a shortening of the small intestine, decreased secretion rate of intestinally derived TRL, and increased lipid retention,^{10,14–16} extending the postprandial period.¹⁷ Therefore, it remains unclear how the kinetics of intestinal triglyceride mass and triglyceride secretion are dysregulated in the postprandial state in insulin resistance.

In the liver, insulin resistance drives upregulation of FoxO1 (forkhead box protein O1) through a lack of phosphorylation. Unlike the FoxO1 pathway, the mTORC1 (mammalian target of rapamycin complex 1) signaling remains insulin-sensitive.¹⁸ As such, prolonged and elevated circulating insulin levels upregulate SREBP-1c (sterol regulatory element binding protein 1c) expression, leading to inappropriately accelerated FA synthesis.¹⁸ Together, enhanced hepatic de novo FA synthesis and increased circulating nonesterified FA (NEFA) provide the substrate for hepatic triglyceride synthesis, which can be stored or packaged in VLDL (very-low-density lipoprotein) particles for secretion.^{18–20} The contribution of this bifurcation in insulin signaling to the kinetics of intestinal

Highlights

- Nobiletin enhances the rate at which intestinal triglyceride-rich lipoprotein are secreted and cleared, independent of GLP-2 (glucagon-like peptide 2) receptor signaling.
- Nobiletin reduces endogenous intestinal fatty acid synthesis by enhancing intestinal insulin signaling and normalizing Srebf1c expression.
- Unlike the liver, nobiletin does not enhance intestinal fatty acid oxidation capacity compared with high-fat, high-cholesterol-fed mice.
- These results demonstrate the effect of high-fat, high-cholesterol diet-induced insulin resistance on intestinal lipid handling and its correction with an insulin-sensitizing compound, nobiletin.

triglyceride mass and postprandial triglyceride secretion is unclear.

Epidemiologically, a higher intake of flavonoids correlates with lower cardiovascular risk.²¹ We and others have reported that nobiletin, a tangerine-derived flavonoid, prevents high-fat diet-induced metabolic dysregulations in WT mice^{22–25} through actions in a variety of tissues in addition to its clock amplitude enhancing properties.²³ Nobiletin administered as either prevention²⁶ or intervention²⁷ treatment in *Ldlr*^{−/−} mice reduces atherosclerosis, VLDL-triglyceride secretion, and hepatic triglyceride accumulation. Mechanistically, nobiletin reduces hepatic FA synthesis and enhances hepatic FA oxidation.^{26,27} Nobiletin also attenuates fasting intestinal triglyceride accumulation in *Ldlr*^{−/−} mice.²⁶ However, the specific mechanism(s) by which nobiletin may influence intestinal lipid metabolism in models of atherogenesis (*Ldlr*^{−/−}) remains unclear. The purpose of these studies was to examine the development of intestinal insulin resistance, intestinal lipid accumulation, and postprandial chylomicron secretion in both male and female mice fed a high-fat, high-cholesterol (HFHC) diet ± nobiletin.

MATERIALS AND METHODS

The data that support the findings of this study are available from the corresponding author upon reasonable request.

Animals and Diets

Male and female *Ldlr*^{−/−}, male C57BL/6J (WT; The Jackson Laboratory, Bar Harbor, MA), and male *Glp1r*^{−/−}*Glp2r*^{−/−} (GLPDRKO) mice²⁸ kindly provided by Dr Daniel Drucker (Toronto, ON) were housed in standard cages at 23°C on a 12-hour light and dark cycle with littermate controls. Mice were cared for following the Canadian Guide for the Care and Use of Laboratory Animals. Approval was obtained for all procedures (Western University-AUP-2016-057, UOHI-AUP-2909). Mice (10–12 weeks) were fed ad libitum one of 3 diets for 10 to 12 weeks: a purified standard laboratory diet (SLD; Teklad-8604,

Envigo, Madison WI), HFHC diet (Teklad-TD09268, Envigo), or HFHC diet supplemented with 0.3% nobiletin (no. 10236-47-2, R&S PharmChem, Hangzhou City, China). The dose of 0.3% has been previously shown to prevent metabolic dysregulation and atherosclerosis in *Ldlr*^{-/-} mice.²⁶ Synthetic mouse GLP (glucagon-like peptide)-2(3-33) (Chi Scientific Maynard, MA) was injected daily (30 ng/d) for 14 days following 10 weeks of HFHC diet.

Blood and Tissue Collection

Metabolic studies, blood collection, fast protein liquid chromatography, and euthanization were as previously described.²⁹ Briefly, the small intestine was divided into duodenum, jejunum, ileum (1:3:2 ratio), and flushed with 0.5 mmol/L sodium taurocholate (37 °C) followed by ice-cold saline. Whole intestinal tissue was used for analysis unless otherwise indicated. Plasma lipids, insulin,²⁶ tissue lipids,²⁹ and gene expression²⁷ were measured as previously described. For GLP-1 measurement (total-K1503PD-2, active-K1526LK, Mesoscale) 5000 KIU/mL Trasylol, 1.2 mg/mL EDTA (ethylenediaminetetraacetic acid), 0.1 nmol/L Diprotin A was added. Please see the Major Resources Table in the [Supplemental Material](#).

Lipid Tolerance Test and Plasma Ultracentrifugation

Mice were fasted for 6 hours and gavaged with 200 μ L olive oil (± 10 μ Ci ³H-triolein, Amersham, Oakville, ON; ± 30 μ g BODIPY-C16_FA, Molecular Probes, Eugene, OR; ± 3 mg acetaminophen). In indicated experiments, mice were also injected with 100 mg/kg poloxamer-407 (P407; IP) 30 minutes before the oil gavage. TRL were isolated by ultracentrifugation (no. 344625 TLA-120.2, Beckman Coulter, Mississauga, ON; 17 000 rpm, 12 °C, 30-minute chylomicrons (<1.006) followed by 40 000 rpm, 12 °C 2-hour VLDL fraction (<1.006)). For fasting samples only, body weight-matched mice were pooled. Triglyceride values in the chylomicron and VLDL fraction were corrected for plasma volume spun and respective fraction volume collected. In WT mice, plasma triglyceride was measured using the Infinity Triglycerides assay. For gastric emptying measurements, plasma acetaminophen was measured (Sekisui Diagnostics, Charlottetown, PE).

Chylomicron Clearance and Glucose Tolerance

Mice were fasted for 5 hours and administered 5310 μ g ULDL (ultra low-density lipoprotein) chylomicrons (LeeBio) in 100 μ L PBS IV, and samples were taken every 2-minute postinjection. An oral glucose tolerance test was performed following a 6-hour fast (1 g/kg body weight), and blood glucose was measured by glucometer (MediCure Canada, Ajax, ON).

Plasma Immunoblotting

Samples from *Ldlr*^{-/-} mice were run on 10% SDS-PAGE gels (Bio-Rad no. 456-1086), transferred onto nitrocellulose membranes, and incubated with apoB primary antibodies (Midland AB_2734118) or albumin (Novus Biologicals NB 600-41532) and secondary IRDye 800CW (no. 925-32214-LI-COR Biosciences, Lincoln, NE), imaged (LI-COR Biosciences Odyssey), and quantitated (ImageStudio Software 5.0). Plasma

from WT mice was run on 4% SDS-PAGE gels, transferred onto nitrocellulose membranes, incubated with apoB antibodies (Midland AB_2734118) and mouse-anti-goat IgG-HRP (Santa Cruz Biotechnologies, sc-2354; RRID:AB_628490), visualized (SuperSignal WestPico PLUS, Thermo Scientific, P134577), imaged (ChemiDoc XRS+; Bio-Rad), and quantitated (ImageLab).

Tissue Immunoblotting

Samples were homogenized in RIPA buffer (Sigma R0278 with P8340, P5726) and dithiothreitol. Protein concentrations were determined as described²⁹ (mTORC1-12.5 μ g, AKT-6.25 μ g, and FoxO1-50 μ g), were visualized using enhanced chemiluminescence reagent (Roche Diagnostics) and quantified using an Imaging Densitometer (GS-700; Bio-Rad).

Jejunal FA/Triglyceride Synthesis and FA Oxidation

FA synthesis was measured 30 minutes following an (intraperitoneal) injection of 20 μ Ci [¹⁻¹⁴C]-acetate (Amersham). Incorporation into FA was measured as described.³⁰ Triglyceride synthesis was measured by incubating jejunal homogenates with [¹⁴C]oleoyl-CoA (Amersham). [³H]cholesteryl-oleate (Amersham) was used as an internal standard.³⁰ For FA oxidation, jejunal mucosa was homogenized. Two μ Ci of [¹⁻¹⁴C]palmitic acid (PerkinElmer: NEC075H250UC) and 150 μ mol/L unlabeled palmitic acid was complexed with 3% FA-free BSA (bovine serum albumin) and ¹⁴CO₂ in the filter pads. The incorporation of tracers was measured by liquid scintillation counting.³⁰

Microscopy

Transmission electron microscopy: jejunal segments were fixed in 1% paraformaldehyde and 1% glutaraldehyde, postfixed in 1% osmium tetroxide, dehydrated, and immersed in acetone. The tissue was infiltrated with epon-araldite resin, embedded, and polymerized (Electron Microscopy Sciences, Hatfield, PA). Sections (Reichert Ultracut) were stained with paraphenylenediamine³¹ and imaged (Leica Aperio At2 slide scanner). Ultrathin sections were stained with Reynold's lead citrate and imaged (Philips 420 TEM, AMT-4KMP XR41S-B camera; Woburn, MA). The identification of CLDs was based on previous characterizations.^{12,32} For fluorescence microscopy, jejunal segments were fixed in 4% paraformaldehyde, incubated in 30% sucrose, embedded in optimal cutting temperature, sectioned (10 μ m), counterstained with DAPI, and imaged (Zeiss AxioScope) where autofluorescence was captured to define tissue outline. CLD area quantification (5 villi/mouse) was performed using CellProfiler (version-4.2.0) using a modified pipeline.³³

Statistical Analysis

Data are presented as mean \pm SEM. Statistical analyses were performed using 1- or 2-way ANOVA (indicated) with post hoc Tukey test following Brown-Forsythe test and Barlett test for normality and equal variance. A *P* < 0.05 was considered significant, and *P* values are listed where appropriate. A notation of NS indicates no statistically significant difference. All data were analyzed using GraphPad Prism 8.

Data and Resource Availability

No applicable resources were generated, and all data generated or analyzed are included in the article and its [Supplemental Material](#).

RESULTS

Nobiletin Attenuates Triglyceride Accumulation in the Circulation and the Jejunum During Fasted and Postprandial States in Male and Female *Ldlr*^{-/-} Mice

Nobiletin has previously been shown to attenuate dyslipidemia in HFHC-fed male WT^{22–25} and *Ldlr*^{-/-} mice.^{26,27} Fast protein liquid chromatography analyses of plasma from both male and female *Ldlr*^{-/-} mice demonstrated elevated triglyceride levels in HFHC-fed mice following a 6-hour fast (Figure 1A and 1B). Nobiletin significantly reduced VLDL-triglyceride in female *Ldlr*^{-/-} mice, however, these levels remained significantly higher than SLD-fed female mice (Figure 1A). Nobiletin significantly reduced VLDL-triglyceride to levels not different from SLD-fed male *Ldlr*^{-/-} controls (Figure 1B). To determine if dietary triglyceride are handled differently in HFHC versus HFHC+nobiletin mice, plasma from *Ldlr*^{-/-} males obtained after 6-hour fast and 2-hour postoil gavage was separated by fast protein liquid chromatography. At 2-hour postgavage, the triglyceride-area under the curve in the fast protein liquid chromatography fractions of male HFHC-fed *Ldlr*^{-/-} mice did not change from the elevated baseline, suggesting delayed intestinal-triglyceride excursion (Figure 1C and 1D). By contrast, the triglyceride-area under the curve of nobiletin-treated male *Ldlr*^{-/-} mice increased significantly from baseline to triglyceride levels significantly lower than HFHC-fed mice (Figure 1C and 1D). HFHC-fed male *Ldlr*^{-/-} mice displayed significantly elevated jejunal triglyceride in the fed state compared with SLD-fed mice, suggesting an accumulation of dietary triglyceride in the jejunum (Figure 1E). By contrast, nobiletin-treated male *Ldlr*^{-/-} mice did not accumulate jejunal triglyceride at any time point (Figure 1E).

To assess an extended view of the postprandial period, a lipid tolerance test (LTT) was performed in male *Ldlr*^{-/-} mice. Despite significantly elevated fasting plasma triglyceride in HFHC-fed mice, the incremental change in plasma triglyceride from the olive oil gavage was not significantly different compared with SLD controls (Figure 1F). Nobiletin treatment elevated triglyceride levels to a greater extent compared with HFHC and SLD-fed mice, particularly at 2-hour postgavage (Figure 1F). In another set of mice, separating triglyceride-rich plasma lipoprotein fractions by ultracentrifugation revealed significantly elevated chylomicron-triglyceride in HFHC-fed mice compared with SLD-fed mice at fasting, 2- and 4-hour postoil (Figure 1G). Chylomicron-triglyceride

levels in nobiletin-treated mice were intermediate and not significantly different from HFHC-fed or SLD-fed mice at any time point (Figure 1G). Plasma VLDL-triglyceride were significantly elevated in HFHC-fed mice at fasting, 1-, 2-, and 4-hour postgavage compared with SLD-fed mice (Figure 1H). Nobiletin treatment led to significantly lower VLDL-triglyceride at fasting, 2-hour, and 4-hour postoil compared with HFHC-fed mice (Figure 1H). Comparisons within diet groups revealed that only HFHC-fed mice displayed significant increases in chylomicron-triglyceride (4 hours) or VLDL-triglyceride (2 and 4 hours) compared with their baselines, suggesting either a delayed secretion or impaired clearance in HFHC-fed mice is prevented by nobiletin.

Nobiletin prevented HFHC-induced weight gain in male and female *Ldlr*^{-/-} mice (Figure S1A and S1C). In male *Ldlr*^{-/-} mice, caloric intake was unchanged across diet groups, however, nobiletin-treated female *Ldlr*^{-/-} mice consumed significantly more calories (≈1.2-fold) than SLD-fed mice (Figure S1B and S1D). As in males,²⁶ nobiletin also prevented hepatic triglyceride accumulation in female *Ldlr*^{-/-} mice (Figure S1E).

Nobiletin Increases the Rate of Intestinal-Triglyceride Secretion in Male WT and *Ldlr*^{-/-} Mice but Not in Female *Ldlr*^{-/-} Mice

To assess intestinal-triglyceride secretion rates, mice were treated with poloxamer-407 (P407) to block lipoprotein lipase (LPL) activity before the LTT. Male *Ldlr*^{-/-} mice additionally received ³H-triolein in the olive oil gavage. HFHC-fed *Ldlr*^{-/-} males displayed significantly lower plasma triglyceride at 1, 2, and 4 hours and radioactivity at 1 and 2 hours, compared with SLD-fed mice (Figure 2A and 2B). Secretion into plasma of triglyceride and radioactivity were significantly higher in nobiletin-treated male *Ldlr*^{-/-} mice compared with HFHC-fed mice (Figure 2A and 2B). Plasma apoB48 levels were not significantly different in nobiletin-treated compared with HFHC-fed mice (Figure 2C). HFHC-fed-female *Ldlr*^{-/-} mice, similar to male *Ldlr*^{-/-} mice, displayed significantly delayed triglyceride secretion (Figure 2D). However, nobiletin treatment did not normalize triglyceride secretion in female mice (Figure 2D). Consistently, HFHC-fed male WT mice had lower plasma triglyceride at 1-hour postgavage compared with SLD controls (Figure 2E). Plasma triglyceride at 1 hour in nobiletin-treated mice was intermediate between HFHC- and SLD-fed mice but was significantly higher over 4 hours (Figure 2E). HFHC-fed WT mice trended to elevated plasma apolipoprotein B-48 (apoB48) signal despite similar plasma triglyceride secretion compared with SLD-fed mice (Figure 2F). Nobiletin treatment attenuated plasma apoB48 secretion compared with HFHC-fed mice to levels similar to SLD-fed mice (Figure 2F).

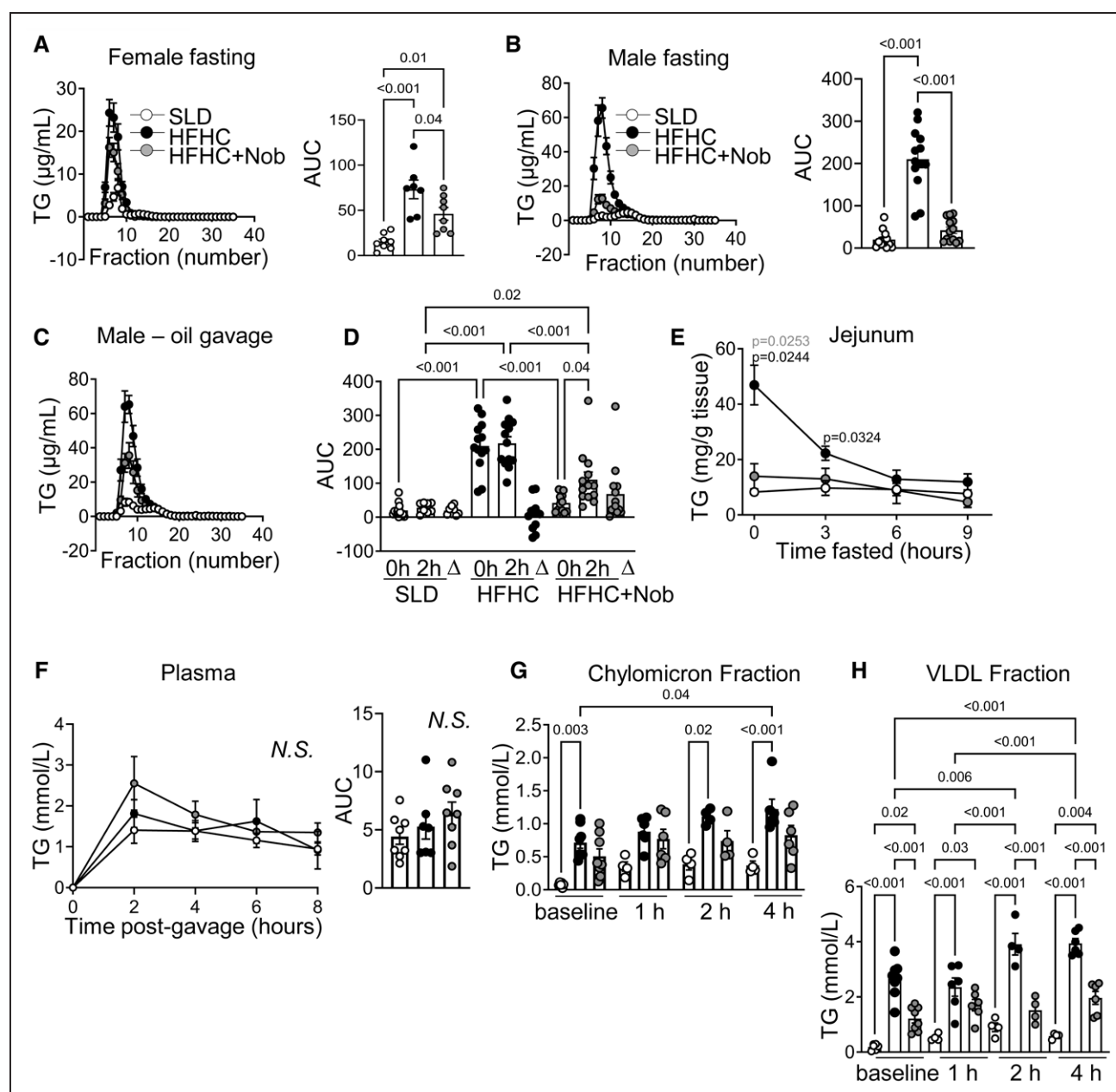


Figure 1. Nobiletin attenuates triglyceride (TG) accumulation in circulation and in the jejunum during the fasted and postprandial state in male *Ldlr*^{-/-} mice.

Fasting (6 h) plasma in (A) female *Ldlr*^{-/-} mice and (B) male *Ldlr*^{-/-} mice for fast protein liquid chromatography (FPLC); TG was measured in each fraction with area under the curve (AUC) calculations of the VLDL (very-low-density lipoprotein)-TG (fractions 5–10; n=8–13/group). C, FPLC-TG 2-h postgavage in the same male mice as in B. D, AUC calculations of fasting and 2-h postgavage VLDL-TG from FPLC fractions and absolute change from baseline (Δ). E, Male *Ldlr*^{-/-} mice were sacrificed in fed state (0) or after 3, 6, and 9 h of fasting for jejunal TG (n=4/time point). F, Lipid tolerance test (LTT) plasma TG with incremental AUC (n=8/time point). In another set of male *Ldlr*^{-/-} mice, fasting plasma from 2 mice per group was pooled and mice were euthanized at 1-, 2-, and 4-h postgavage for ultracentrifugation (n=4–6/time point). TG measured in the (G) chylomicron- and (H) VLDL-fractions. Values are mean±SEM. ANOVA with post hoc Tukey test was used to calculate statistical significance and P values are labeled in each graph. In secretion curves (E and F) statistical differences over time were determined by 2-way ANOVA, where P values for each time point are indicated for statistical differences between high-fat, high-cholesterol (HFHC)+nobiletin and HFHC-fed (gray) and standard laboratory diet (SLD)-fed compared with HFHC-fed (black). NS indicates non significant.

Nobiletin Increases the Triglyceride Content of Chylomicron Particles in Male but Not Female *Ldlr*^{-/-} Mice

To determine if nobiletin alters the number or triglyceride enrichment of TRL-particles secreted, TRL fractions

were isolated at fasting and 2-hour postoil and P407. HFHC-fed-male *Ldlr*^{-/-} mice displayed significantly reduced chylomicron-triglyceride secretion compared with SLD-fed mice (Figure 3A). Nobiletin treatment restored chylomicron-triglyceride secretion to a rate not significantly different from SLD-fed mice (Figure 3A).

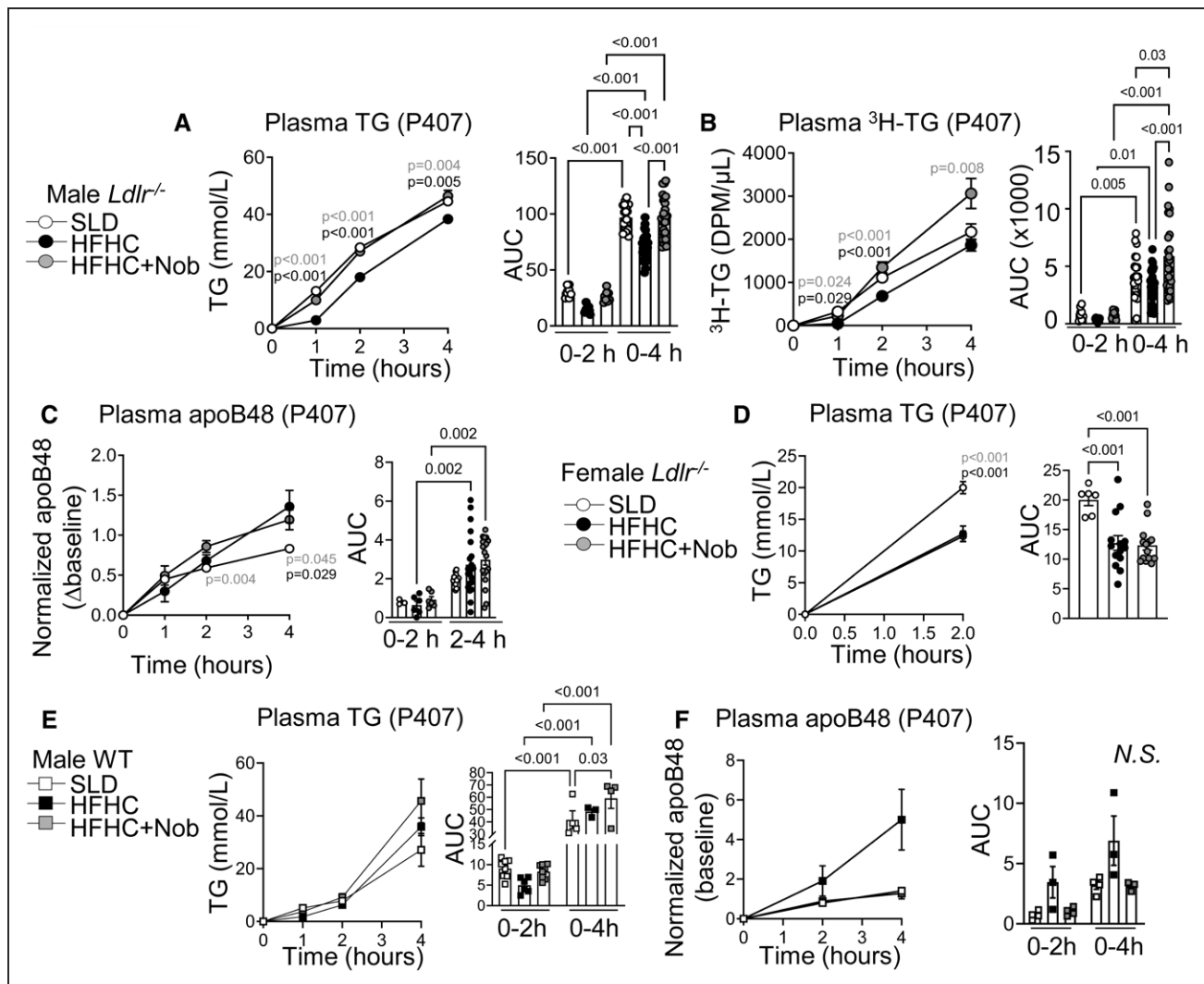


Figure 2. Nobiletin increases the rate of intestinal-triglyceride (TG) secretion in male *Ldlr*^{-/-} mice and wild-type (WT) male mice but not in female *Ldlr*^{-/-} mice.

Lipid tolerance test (LTT) was performed in male *Ldlr*^{-/-} mice with P407 and olive oil containing [³H]triolein. LTT plasma (A) TG and (B) [³H]TG (n=8–37/time point) displayed as a difference from baseline with area under the curve (AUC) calculations on the right. C, LTT plasma apoB48 (n=4–26/time point) displayed as a difference from baseline where samples were normalized to albumin, and this ratio was normalized to the 2-h apoB48/albumin signal of a standard laboratory diet (SLD)-fed mouse, run on each gel (n=4–27/time point) with AUC calculations. LTT was performed in female *Ldlr*^{-/-} mice with P407. D, LTT plasma TG displayed as a difference from baseline with AUC calculations. LTT in male WT mice with P407 and olive oil containing BODIPY-C16-fatty acid (FA). LTT (E) plasma TG. F, Plasma apoB48 (n=3–4/group) with AUC calculations. Values are mean±SEM. ANOVA with post hoc Tukey test was used to calculate statistical significance and P values are labeled in each graph. In secretion curves statistical differences over time were determined by 2-way ANOVA. In A, B, E, and F, P values for each time point are indicated for statistical differences between high-fat, high-cholesterol (HFHC)+nobiletin and HFHC-fed (gray) and SLD-fed compared with HFHC-fed (black). In C and D, P values indicate statistical differences between HFHC+nobiletin and SLD (gray) and HFHC compared with SLD (black). NS indicates non significant.

Despite similar fasting chylomicron-triglyceride values between diet groups (Figure 3A), HFHC-fed mice displayed significantly elevated fasting apoB48 (Figure 3B). Nobiletin-treated mice were the only diet group to display a significant increase in chylomicron-apoB48 from baseline (Figure 3B). Triglyceride:apoB48 calculations (particle size) revealed a significant postprandial enrichment in all diet groups (Figure 3C). Still, postoil chylomicron-triglyceride:apoB48 from HFHC-fed mice was significantly lower compared with SLD-fed mice (Figure 3C). Nobiletin treatment led to significantly higher chylomicron-triglyceride:apoB48 relative to HFHC-fed mice, but

it did not entirely correct this defect. In female *Ldlr*^{-/-} mice fed a HFHC or SLD, the patterns of response for secretion of chylomicron-triglyceride, chylomicron-apoB48, and chylomicron-triglyceride:apoB48 (Figure 3D through 3F) were similar to those of male *Ldlr*^{-/-} mice (Figure 3A through 3C); however, in contrast to male *Ldlr*^{-/-} mice, nobiletin did not prevent HFHC diet-induced changes to these parameters (Figure 3D through 3F). Postoil gavage, VLDL-triglyceride levels in male *Ldlr*^{-/-} mice increased significantly at 2 hours in all diet groups compared with their respective baseline (Figure 3G). Nobiletin treatment led to significantly greater VLDL-triglyceride secretion

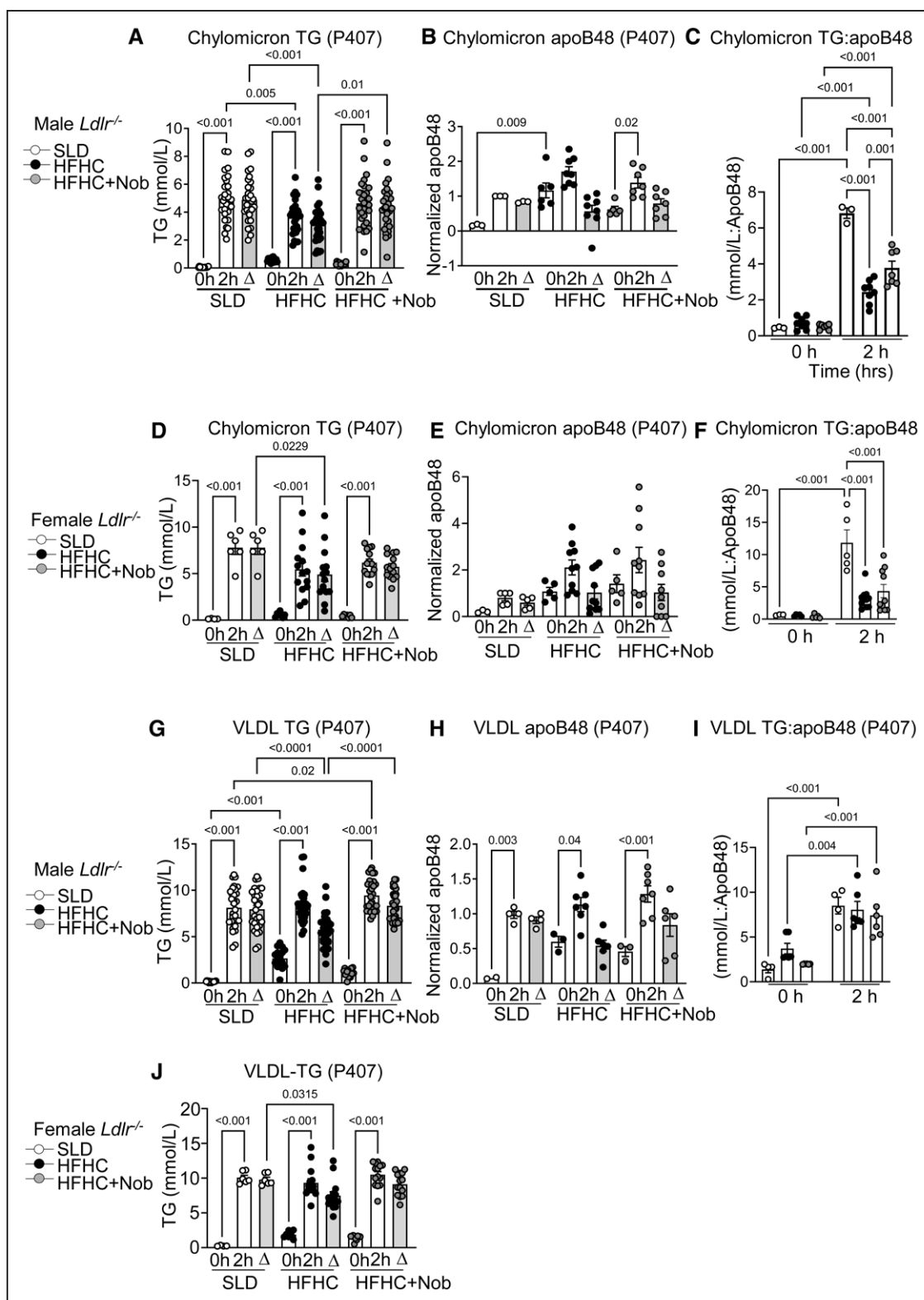


Figure 3. Nobiletin increases the triglyceride (TG) content of chylomicron particles in male but not female *Ldlr*^{-/-} mice.

Lipid tolerance test (LTT) with P407 was performed in *Ldlr*^{-/-} mice. Fasting plasma from 2 mice per group was pooled and mice were euthanized 2-h postgavage (n=16–30/time point) for plasma ultracentrifugation. In male *Ldlr*^{-/-} mice, (A) chylomicron-TG, (B) chylomicron-apoB48, and (C) ratio of chylomicron-TG to chylomicron-apoB48 signal. In female *Ldlr*^{-/-} mice, (D) chylomicron-TG, (E) chylomicron-apoB48, and (F) ratio of chylomicron-TG to chylomicron-apoB48. In male *Ldlr*^{-/-} mice, (G) VLDL (very-low-density lipoprotein)-TG, (H) VLDL-apoB48 signal, and (I) ratio of VLDL-TG to apoB48 signal. In female *Ldlr*^{-/-} mice, (J) VLDL-TG. Values are mean±SEM. ANOVA with post hoc Tukey test was used to calculate statistical significance and *P* values are labeled in each graph when appropriate. HFHC indicates high-fat, high-cholesterol; and SLD, standard laboratory diet.

compared with HFHC-fed male *Ldlr*^{-/-} mice (Figure 3G). VLDL-apoB48 secretion and VLDL-triglyceride:apoB48 ratios were similar among groups (Figure 3H and 3I). In female *Ldlr*^{-/-} mice, HFHC-feeding led to significantly lower VLDL-triglyceride secretion at 2 hours compared with SLD-fed controls, while nobiletin-treated mice displayed an intermediate VLDL-triglyceride secretion rate that was not different from HFHC fed or SLD controls (Figure 3J).

TRL Clearance Is Elevated by Nobiletin

To estimate the plasma triglyceride clearance rate in male mice, we compared triglyceride secretion rates with and without P407 treatment in the same set of male *Ldlr*^{-/-} mice. We observed a significantly lower clearance rate in HFHC-fed mice compared with SLD controls (Figure 4A and 4B). Nobiletin treatment led to a significantly higher clearance rate compared with HFHC-fed mice (Figure 4A and 4B). In male WT mice, the same significantly lower clearance rate in HFHC-fed mice compared with SLD-fed controls was observed (Figure 4C and 4D), whereas triglyceride clearance in nobiletin-treated WT mice was intermediate between and not statistically different from the other 2 groups (Figure 4D). A more direct assessment of chylomicron-triglyceride clearance was measured in all 3 dietary groups of WT male mice (Figure 4E). Triglyceride mass rapidly decreased in all groups within the first 2 minutes. Area under the curve calculations revealed enhanced triglyceride clearance in nobiletin-treated mice compared with HFHC-fed mice (Figure 4E). In WT male mice, *Ldlr* mRNA expression in jejunum and liver was not different among groups (Figure 4F and 4G). Jejunal *Apoc3* mRNA, an inhibitor of LPL activity and regulator of hepatic TRL clearance,³⁴ was significantly higher in HFHC-fed WT male mice compared with both SLD-fed and nobiletin-treated mice (Figure 4H). Moreover, we observed significantly greater gastric emptying in nobiletin-treated WT male mice compared with SLD controls, suggesting enhanced nutrient transit into circulation (Figure 4I). Therefore, in addition to enhanced intestinal-triglyceride secretion, nobiletin accelerated plasma triglyceride clearance.

Nobiletin Attenuates Intestinal Lipid Storage in Male but Not Female *Ldlr*^{-/-} Mice

During fat absorption, resynthesized triglyceride within enterocytes can be stored in CLDs as reservoirs for later export.³⁵ Moreover, high fat-fed mice have been reported to have more abundant and larger intestinal CLDs postoil gavage compared with SLD-fed mice.^{16,36} In male *Ldlr*^{-/-} mice, levels of the radiolabel 2 hours post-³H-triolein/oil gavage was not significantly different among diet groups, suggesting that tracer uptake was similar, however, differences in tracer metabolism cannot be excluded

(Figure 5A). Total jejunal triglyceride mass was significantly higher in HFHC-fed *Ldlr*^{-/-} male mice 2-hour postgavage compared with SLD-fed controls (Figure 5B). In contrast, jejunal triglyceride mass in nobiletin-treated mice was significantly lower compared with HFHC-fed mice (Figure 5B). Intestinal triglyceride levels were similar among groups by 4-hour postoil gavage (Figure S1F). In contrast to male *Ldlr*^{-/-} mice, jejunal triglyceride mass 2-hour postgavage was not significantly different among groups in female *Ldlr*^{-/-} mice (Figure 5C).

Neutral lipid accumulation was observed in light micrographs of enterocytes 2-hour postoil gavage of male *Ldlr*^{-/-} HFHC-fed mice, and this signal appeared diminished in nobiletin-treated mice (Figure 5D). Electron micrographs revealed an abundance of large CLDs in enterocytes of a HFHC-fed *Ldlr*^{-/-} male mouse (Figure 3E). By contrast, large CLDs appeared less frequent with nobiletin treatment while smaller CLDs were abundant (Figure 3E). In male WT male mice, jejunal sections 2-hour post-BODIPY-C16 gavage revealed dietary fat-derived CLDs in all diet groups (Figure 5F). Image quantification of BODIPY-CLD area revealed a significantly greater CLD size in HFHC-fed mice compared with SLD-fed controls (Figure 5G). Lipid droplet size in nobiletin-treated mice was not statistically different from HFHC- or SLD-fed mice (Figure 5G). Quantification of BODIPY-CLD area 4-hour postgavage revealed no significant differences among groups (Figure S1G and S1H).

Gene expression of enzymes involved in intestinal FA trafficking, triglyceride synthesis, and chylomicron assembly⁵ was measured in jejunal tissue postoil gavage. Jejunal *Srebf1c* mRNA expression was significantly higher in HFHC-fed male and female *Ldlr*^{-/-} mice and male WT mice compared with SLD-fed mice (Figure 5H). Nobiletin treatment led to significantly lower *Srebf1c* mRNA expression but only in male *Ldlr*^{-/-} mice (Figure 5H). *Plin2* is involved in lipid absorption and CLD stabilization,³⁷ and compared with SLD, nobiletin led to significantly higher postprandial jejunal mRNA expression of *Plin2* in all models tested (Figure 5I). *Atgl* mediates triglyceride hydrolysis from CLDs, and its jejunal expression is reduced in high fat-fed WT mice 2-hour postoil gavage.¹⁰ Consistent with this, *Atgl* mRNA expression was significantly lower in male and female *Ldlr*^{-/-} HFHC-fed mice compared with SLD controls (Figure 5J). Nobiletin did not significantly change *Atgl* mRNA expression in male *Ldlr*^{-/-} mice, whereas in female *Ldlr*^{-/-} mice, this expression was significantly lower compared with in SLD-fed mice (Figure 5J). In male WT mice, no differences in jejunal *Atgl* mRNA were observed among groups (Figure 5J). In male *Ldlr*^{-/-} mice, postprandial mRNA expression of jejunal *Cd36*, *Dgat2*, and *Mttp* were not different among groups (Figure S1I). In male WT mice, jejunal *ApoB48*, *Fabp2*, and *Mogat2* mRNA expression were not significantly different among groups (Figure S1J).

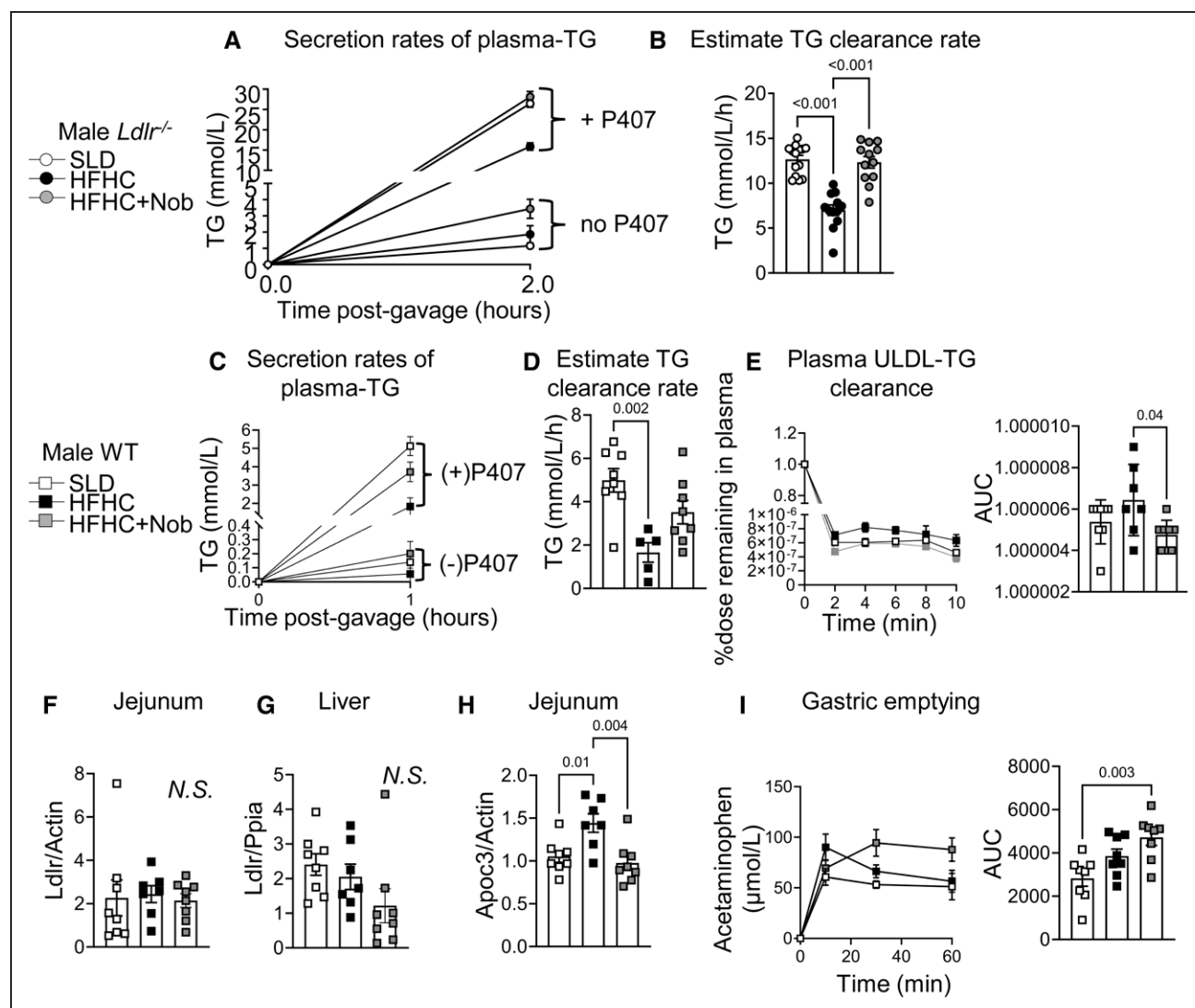


Figure 4. Assessing chylomicron clearance particle rates in male *Ldlr*^{-/-} and male wild-type (WT) mice.

A, Comparison of plasma triglyceride (TG) secretion rates in male *Ldlr*^{-/-} mice treated \pm P407 ($n=12-14$ /group). **B**, Estimated plasma TG clearance rate calculated from the difference in TG secretion \pm P407. **C**, Comparison of plasma TG secretion rates and **(D)** estimated plasma TG clearance rate in male WT mice without P407 (**bottom**) and with P407 (**top**; $n=7-8$). **E**, Male WT mice were injected with human chylomicrons (intravenous) following a 5-h fast and blood samples were taken for TG measurements, normalized to 4% body weight, and area under the curve (AUC) calculations. Postprandial mRNA expression of *Ldlr* in **(F)** jejunum and **(G)** liver samples. **H**, Postprandial jejunal mRNA expression of *Apoc3*. **I**, Gastric emptying in male WT mice was assessed during an lipid tolerance test (LTT; +3 mg acetaminophen) by measuring plasma acetaminophen postgavage and AUC calculations. Values are mean \pm SEM. ANOVA with post hoc Tukey test was used to calculate statistical significance and *P* values are labeled in each graph when appropriate. HFHC indicates high-fat, high-cholesterol; NS, non significant; and SLD, standard laboratory diet.

Nobiletin Does Not Attenuate Fasting Lipid Accumulation by Increasing FA Oxidation

Consistent with the time-course shown in Figure 1 and previous results,²⁶ at 6 hours of fasting, representative oil-red-O staining of jejunal sections reveal marked neutral lipid accumulation in male *Ldlr*^{-/-} HFHC-fed mice but not in SLD-fed or nobiletin-treated mice (Figure 6A). Nobiletin treatment led to lower fasting jejunal triglyceride in male (significantly) and female (trend, $P=0.0628$) *Ldlr*^{-/-} mice compared with mice fed the HFHC diet alone (Figure 6B and 6C). HFHC feeding led to

significantly higher fasting jejunal cholesteryl ester in male (≈ 5 -fold) and female (≈ 1.7 -fold) *Ldlr*^{-/-} mice compared with SLD-fed mice, which was significantly reduced by nobiletin treatment but only in male *Ldlr*^{-/-} mice (Figure 6D and 6E). Nobiletin reduces HFHC diet-induced hepatic triglyceride mass by increasing FA oxidation in the liver.²⁶ To determine if nobiletin attenuates intestinal lipid accumulation in male *Ldlr*^{-/-} mice through a similar mechanism, jejunal FA oxidation was measured ex vivo. Jejunal FA oxidation was significantly higher in both HFHC-fed and nobiletin-treated *Ldlr*^{-/-} male mice compared with SLD-fed controls

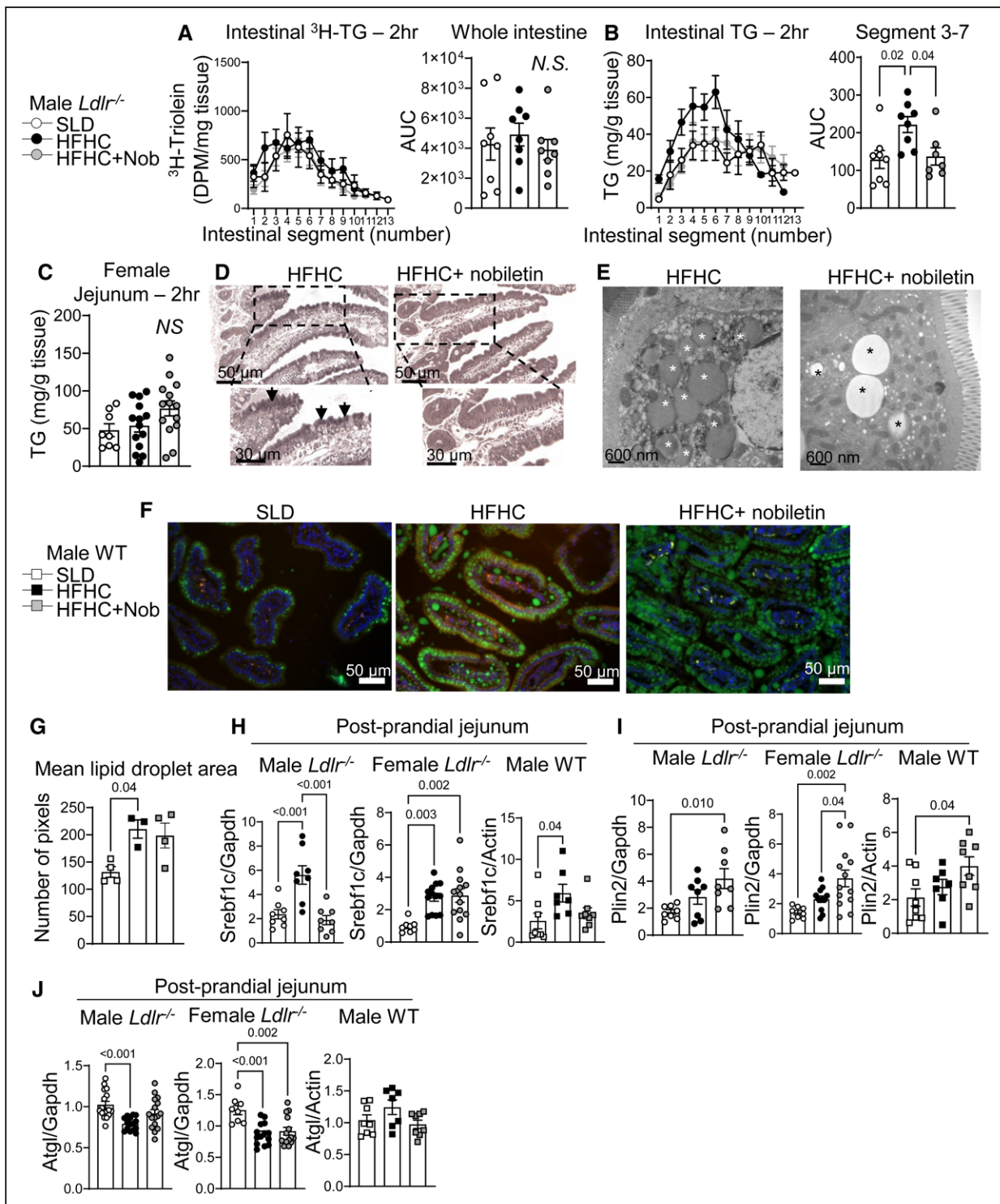


Figure 5. Nobiletin attenuates postprandial lipid accumulation in male but not female *Ldlr*^{-/-} mice or male wild-type (WT) mice.

Lipid tolerance test (LTT) in male and female *Ldlr*^{-/-} mice with P407; male mice received a gavage of olive oil containing [³H]triolein. **A**, Distribution of [³H]triolein uptake or (B) triglyceride (TG) mass along the small intestine axis from pylorus to the ileocecal junction 2-h postgavage and area under the curve (AUC) calculations in male *Ldlr*^{-/-} mice (n=7–8/group) and (C) in the jejunum of female *Ldlr*^{-/-} mice. **D**, Representative paraffin-embedded micrographs of jejunal segments (2-h postgavage); arrows point to lipid droplets. **E**, Representative electron micrographs of jejunal segments (n=2/group; 2-h postgavage); stars indicate cytoplasmic lipid droplets. LTT in male WT mice with P407 and olive oil containing BODIPY-C16 fatty acid (FA). **F**, Representative images of jejunal sections 2-h postgavage visualizing BODIPY-labeled lipid droplets, DAPI-stained nuclei, and tissue autofluorescence (orange). **G**, Quantification of lipid droplet area in jejunal epithelium (n=3–4). **H**, Postprandial jejunal expression of *Srebf1c*, (I) *Plin2*, (J) *Atgl* mRNA in male and female *Ldlr*^{-/-} mice and male WT mice. Values are mean±SEM. ANOVA with post hoc Tukey test was used to calculate statistical significance and *P* values are labeled in each graph when appropriate. HFHC indicates high-fat, high-cholesterol; NS, non significant; and SLD, standard laboratory diet.

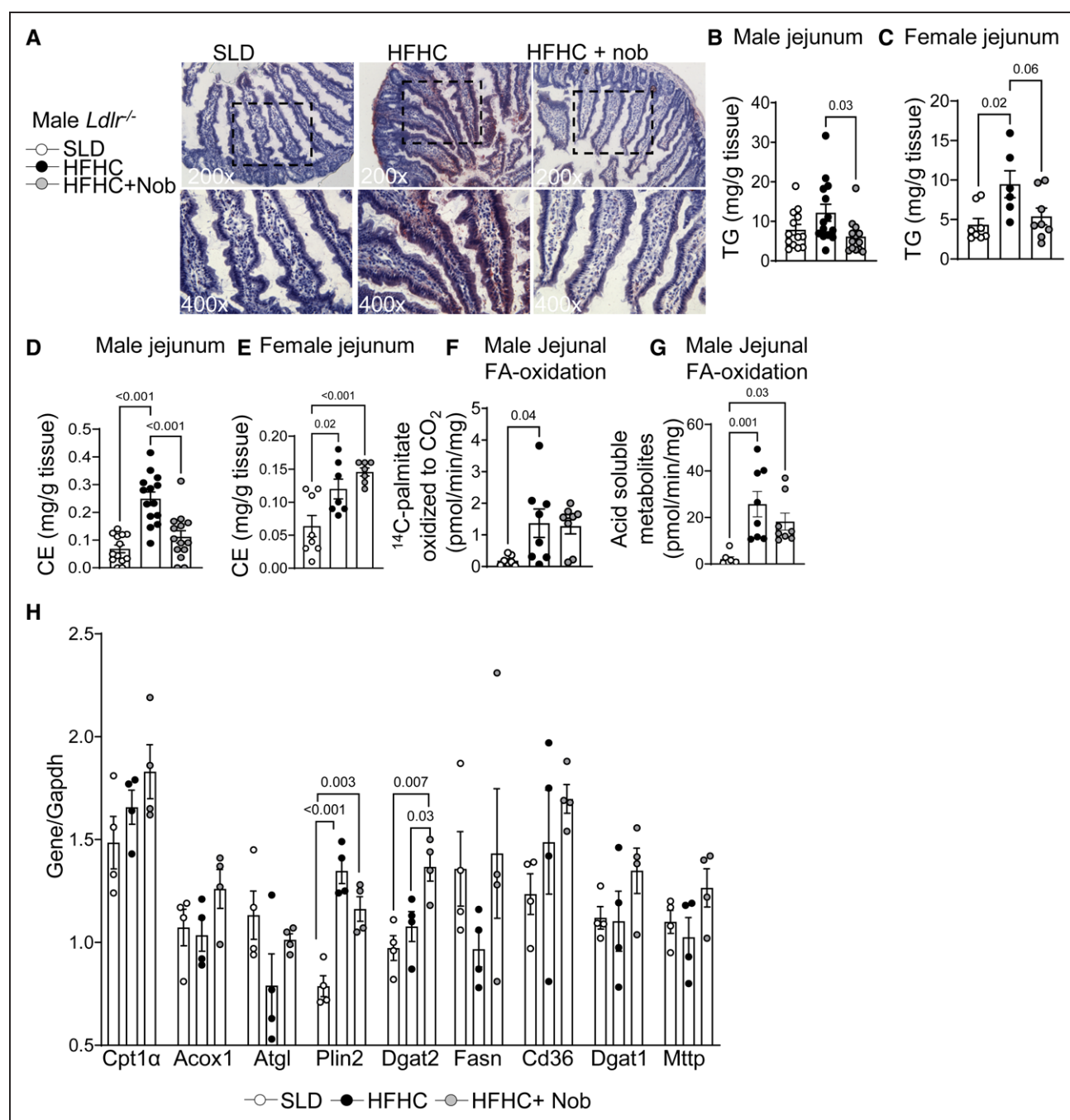


Figure 6. Nobiletin prevents high-fat, high-cholesterol (HFHC) diet-induced jejunal lipid accumulation in *Ldlr*^{-/-} mice independent of fatty acid (FA) oxidation.

Mice were fasted for 6 h. **A**, Representative Oil-Red-O staining of jejunal sections in male *Ldlr*^{-/-} mice. Jejunal triglyceride (TG) mass in **(B)** male ($n=13-14/\text{group}$) and **(C)** female *Ldlr*^{-/-} mice ($n=6-8/\text{group}$). Jejunal cholesteryl ester (CE) mass in **(D)** male and **(E)** female *Ldlr*^{-/-} mice. Jejunal FA oxidation was assessed in male *Ldlr*^{-/-} mice by measuring **(F)** ¹⁴CO₂ released and **(G)** acid soluble metabolites ($n=7-8/\text{group}$). **H**, Fasting jejunal mRNA expression of *Cpt1α*, *Acox1*, *Atgl*, *Plin2*, *Dgat2*, *Fasn*, *Cd36*, *Dgat1*, and *Mttp* ($n=4/\text{group}$). Values are mean \pm SEM. ANOVA with post hoc Tukey test was used to calculate statistical significance and *P* values are labeled in each graph when appropriate. SLD indicates standard laboratory diet.

(Figure 6F and 6G). In *Ldlr*^{-/-} male mice, fasting (6 hours) jejunal mRNA expression of genes related to FA oxidation, *Cpt1α*, *Acox1*, and *Atgl* mRNA were not significantly different among diet groups (Figure 6H). Jejunal *Plin2* mRNA was significantly higher in fasted HFHC-fed and nobiletin-treated mice compared with

SLD-fed controls (Figure 6H). Nobiletin treatment led to significantly higher *Dgat2* mRNA expression compared with both HFHC- and SLD-fed mice, whereas no significant differences in mRNA expression of other lipid synthesis genes such as *Fasn*, *Cd36*, *Dgat1*, and *Mttp* were observed among groups (Figure 6H).

Nobiletin Improves Intestinal Insulin Signaling in *Ldlr*^{-/-} Mice and Decreases De Novo Lipogenesis

To determine if intestinal insulin resistance contributes to the observed intestinal lipid accumulation in HFHC-fed male *Ldlr*^{-/-} mice, we assessed intestinal insulin signaling in response to physiological insulin using a 6-hour fasting, 2-hour refeeding protocol. Plasma insulin increased in all groups upon refeeding and to a greater extent in nobiletin-treated mice compared with SLD- and HFHC-fed mice (Figure 7A). Nobiletin led to significantly lower fasting plasma NEFA compared with HFHC-fed mice (Figure 7B). In HFHC-fed mice, refeeding failed to suppress plasma NEFA, whereas with nobiletin, NEFA suppression was similar to levels observed in SLD-fed mice (Figure 7B). Jejunal AKT phosphorylation increased in all groups with refeeding, and to a greater extent with nobiletin treatment compared with HFHC-fed mice, consistent with nobiletin's insulin-sensitizing properties (Figure 7C). Jejunal FOXO1 phosphorylation did not significantly change in SLD-fed or HFHC-fed mice with refeeding (Figure 7D). In contrast, HFHC+nobiletin refeeding significantly increased jejunal FOXO1 phosphorylation from baseline (Figure 7D). Both fasting and refeeding mTORC1 phosphorylation levels were not significantly different among diet groups (Figure 7E). However, the mRNA expression of a downstream target of mTORC1, *Srebf1c*, increased significantly with refeeding in both HFHC-fed and nobiletin-treated mice (Figure 7F), however, the increase with nobiletin was significantly attenuated compared with HFHC alone (Figure 7F). HFHC-feeding led to significantly higher jejunal FA synthesis 1.6-fold compared with SLD in male mice (Figure 7G), which was significantly attenuated by nobiletin. Jejunal triglyceride synthesis, evaluated *ex vivo*, was significantly higher in both HFHC-fed and nobiletin-treated mice compared with that in SLD-fed mice (Figure 7H). In female *Ldlr*^{-/-} mice, there was no significant difference in jejunal triglyceride synthesis capacity among diet groups (Figure 7I). Collectively, these results suggest that in male *Ldlr*^{-/-} mice nobiletin enhances intestinal insulin sensitivity to reduce *Srebf1c*-mediated jejunal FA synthesis.

Nobiletin Prevents HFHC Diet-Induced Shortening of The Small Intestine and Increases Plasma GLP-1

We next evaluated nobiletin as a nutritional signal to increase the secretion of gut hormones that also regulate intestinal lipid metabolism,⁶ namely, GLP-1 and GLP-2. Reliable assays for plasma GLP-2 in mice are not currently available.³⁸ However, as GLP-1 and GLP-2 are processing products of the same gene, an increase in plasma GLP-1 is likely accompanied by increased GLP-2. In male

Ldlr^{-/-} mice, total plasma GLP-1 increased significantly 10-minute posttoil in all diet groups, however, absolute levels were significantly greater with nobiletin (Figure 8A). In female *Ldlr*^{-/-} mice, fasting plasma GLP-1 was not different (Figure 8B). As previously reported,^{39,40} HFHC-feeding significantly reduced small intestinal weight in male and female *Ldlr*^{-/-} mice, which was prevented with nobiletin treatment (Figure 8C and 8D), consistent with increased GLP-1⁴¹ and GLP-2 intestinotrophic action.⁴² HFHC-feeding significantly shortened small intestinal length (Figure 8E and 8F), whereas nobiletin attenuated this shortening in both sexes in *Ldlr*^{-/-} mice (Figure 8E through 8G). In male WT mice, plasma active GLP-1 significantly increased in both HFHC-fed and nobiletin-treated mice posttoil, however, no significant differences in absolute levels were observed (Figure 8H). HFHC-feeding also shortened the small intestinal length of male WT mice (Figure 8I) and displayed a non significant ($P=0.07$) trend for increased jejunal villi length (Figure 8J). Overall, these data suggested increased GLP-1 and GLP-2 as a potential mechanism of nobiletin treatment. Since nobiletin treatment enhanced intestinal-triglyceride secretion in male *Ldlr*^{-/-} mice and that GLP-2R (glucagon-like peptide-2 receptor) signaling also enhances dietary triglyceride mobilization,⁴³ we hypothesized that nobiletin increased TRL secretion in a GLP-2-dependent manner.

Nobiletin Does Not Require Intact GLP-2R Signaling to Increase the Rate of Intestinal-Triglyceride Secretion

To determine if nobiletin enhanced endogenous GLP-2R signaling, 2 dietary groups of male *Ldlr*^{-/-} mice were treated with the GLP-2R antagonist, GLP-2 (3-33), or PBS for 14 days. GLP-2(3-33) did not affect body weight (Figure S2A and S2B). GLP-2(3-33) reduced jejunal villi length in HFHC-fed mice compared with PBS controls (Figure S2C), as previously reported,⁴⁴ suggesting that the GLP-2(3-33) was systemically active. GLP-2(3-33) did not change jejunal villi length in nobiletin-treated mice compared with PBS controls (Figure S2C). GLP-2(3-33), previously shown to worsen hepatic steatosis,⁴⁵ led to higher hepatic triglyceride mass in HFHC-fed mice and nobiletin-treated mice, but not significantly, and did not affect hepatic cholesteryl ester or free cholesterol (Figure S2D through S2F). Upon LTT with P407 treatment, nobiletin led to significantly greater chylomicron-triglyceride secretion compared with SLD-fed mice and HFHC-fed mice, but this difference was lost with GLP-2(3-33) treatment (Figure 9A). Nobiletin led to significantly greater VLDL-triglyceride secretion compared with HFHC-fed mice, but this difference was lost with GLP-2(3-33) treatment (Figure 9B). GLP-2(3-33) treatment did not significantly change fasting or postprandial chylomicron-apoB48 levels within diet groups (Figure 9C). GLP-2(3-33) did not impact nobiletin's ability to reduce postprandial jejunal

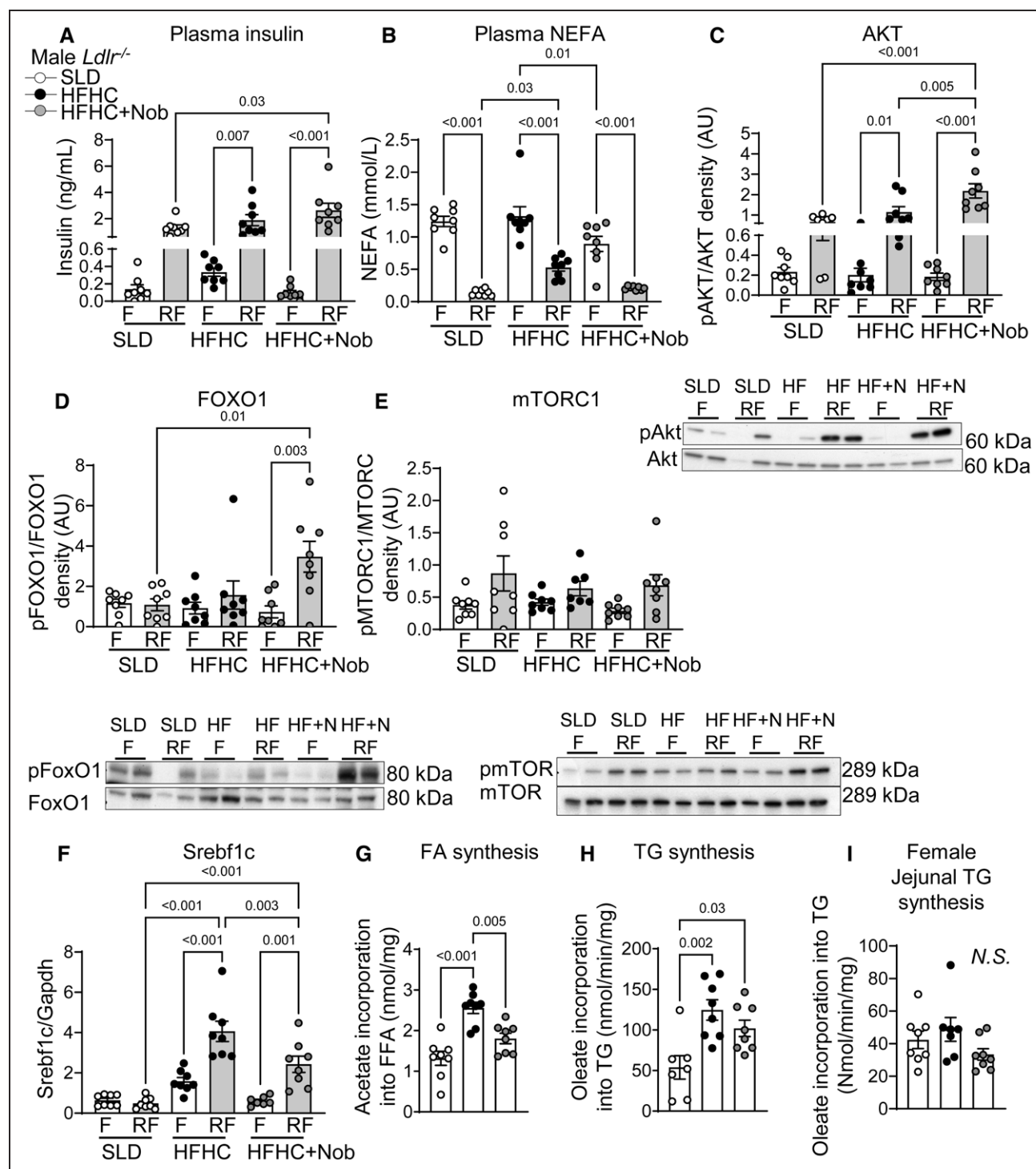


Figure 7. Nobiletin improves dysregulated intestinal insulin signaling.

Male *Ldlr*^{-/-} mice were fasted for 6 h and euthanized in the fasted (F) or 2 h after refeeding (RF) their respective diets. Plasma (A) insulin and (B) nonesterified fatty acid (NEFA) levels (n=8/group). Jejunal (C), AKT (D) FoxO1 (forkhead box O1), and (E) mTORC1 (mammalian target of rapamycin complex 1) presented as a ratio of phosphorylated to total protein (n=8/group). F, Jejunal Srebf1c expression (n=7–8/group). G, Jejunal FA synthesis, determined by measuring ¹⁴C-acetic acid incorporation into FA (n=8/group). Jejunal triglyceride (TG) synthesis, determined by ¹⁴C-oleate incorporation (n=8/group) in (H) male and (I) female *Ldlr*^{-/-} mice. Values are mean±SEM. ANOVA with post hoc Tukey test was used to calculate statistical significance, and P values are labeled in each graph when appropriate. HFHC indicates high-fat, high-cholesterol; NS, non significant; and SLD, standard laboratory diet.

triglyceride mass and increase small intestinal length (Figure 9D and 9E). However, the diet-induced differences in small intestinal weight were lost (Figure 9F). Collectively,

these results suggest that 14 days of GLP-2R antagonism did not significantly impact postprandial hepatic, intestinal, or plasma lipid metabolism in male *Ldlr*^{-/-} mice.

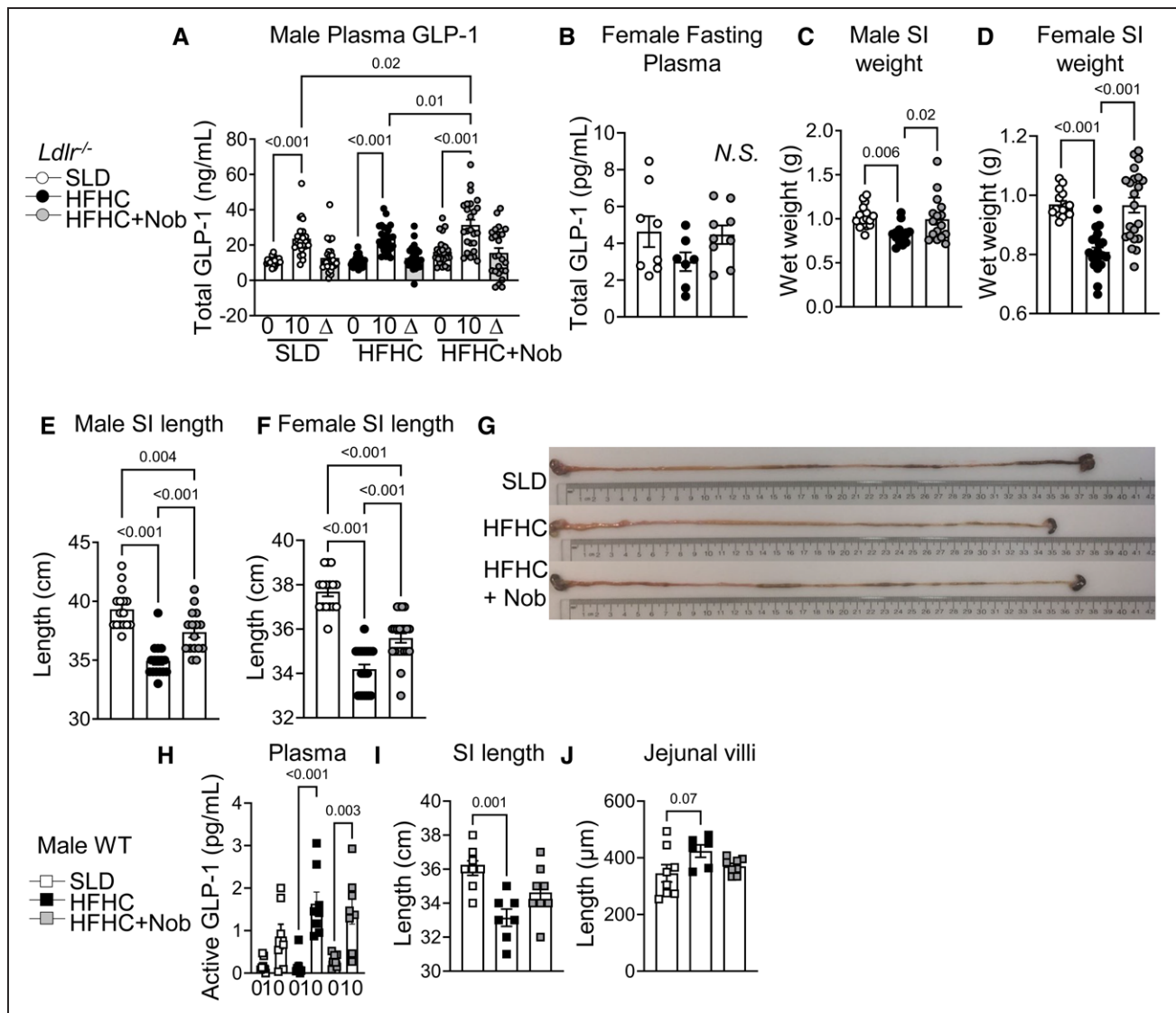
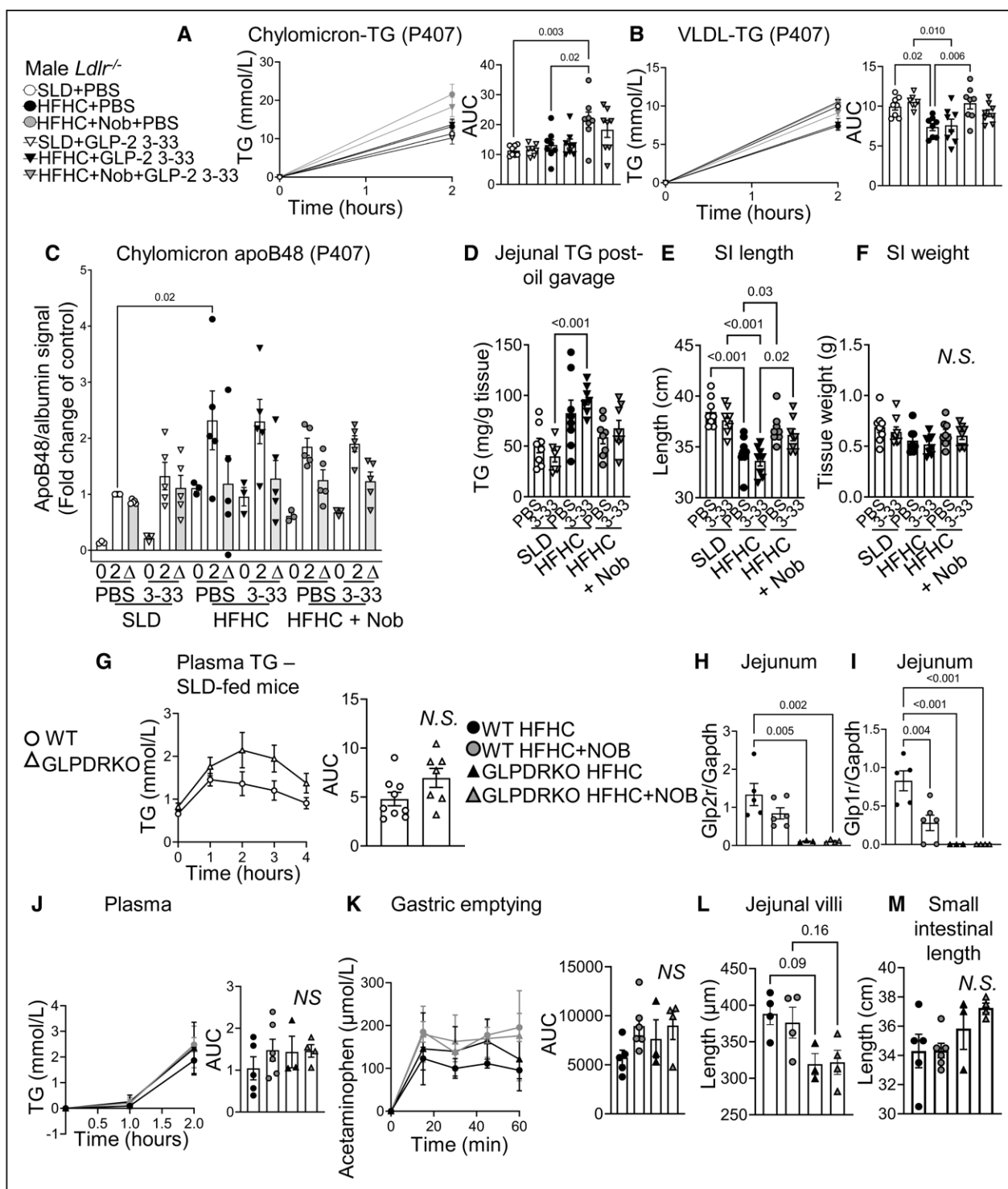


Figure 8. Nobiletin increases plasma GLP-1 (glucagon-like peptide-1) and improves physical gut parameters in male and female *Ldlr*^{-/-} mice and in male wild-type (WT) mice.

Plasma GLP-1 was measured following a 6-h fast (0) and 10-min postgavage (10), and the difference from baseline was calculated (Δ) in (A) male *Ldlr*^{-/-} mice (n=12–14/time point). Fasting (6 h) GLP-1 was measured in (B) female *Ldlr*^{-/-} mice (n=6–9/group). Small intestinal weight in (C) male and (D) female *Ldlr*^{-/-} mice (n=14–20/group). Small intestinal length in (E) male (F) female *Ldlr*^{-/-} mice. G, Representative images of small intestines from male *Ldlr*^{-/-} mice. H, Active GLP-1 in plasma from fasting blood samples (6 h) and 10-min postgavage in male WT mice (n=8/group). Small intestinal (I) length and (J) jejunal villi length in male WT mice. Values are mean±SEM. ANOVA with post hoc Tukey test was used to calculate statistical significance, and P values are labeled in each graph when appropriate. HFHC indicates high-fat, high-cholesterol; NS, non significant; and SLD, standard laboratory diet.

To evaluate the requirement for proglucagon peptide signaling pathways for nobiletin to improve intestinal lipid metabolism in WT male mice, we treated HFHC-fed *Glp1r*^{-/-}*Glp2r*^{-/-} (GLPDRKO) male mice with nobiletin. Before HFHC-feeding, GLPDRKO mice on a SLD displayed a trend for elevated intestinal-triglyceride secretion compared with WT controls (Figure 9G). GLPDRKO displayed worsened glucose tolerance compared with HFHC-fed WT mice, which was significantly improved by nobiletin (Figure S2G). Nobiletin attenuated HFHC diet-induced weight gain and adiposity in WT (significantly) and GLPDRKO mice (trend; Figure S2H and S2I). Jejunal

mRNA expression of *Glp2r* and *Glp1r* were low or undetectable in this model (Figure 9H and 9I), confirming the knockout. Mice were challenged to an LTT, where the responses were similar between diet groups or genotypes (Figure 9J). Nobiletin treatment trended to enhanced gastric emptying, independent of GLP-1R/GLP-2R signaling (Figure 9K). Loss of GLP-1R/GLP-2R signaling shortened jejunal villi length and enhanced intestinal length, independent of nobiletin treatment (Figure 9L and 9M). Overall, these data suggest that in *Ldlr*^{-/-} or WT mice nobiletin treatment does not require GLP-1R or GLP-2R signaling to prevent HFHC-induced metabolic dysregulation.



DISCUSSION

Previous studies have demonstrated that nobiletin lowered fasting plasma triglyceride levels through reduced apoB-VLDL secretion, restored hepatic insulin sensitivity, reduced hepatic FA synthesis, enhanced hepatic FA oxidation, and prevented HFHC diet-induced body weight gain in male WT mice^{22–25} and male *Ldlr*^{−/−} mice²⁶ as well as atherosclerosis in male *Ldlr*^{−/−} mice.^{26,27} Given the renewed appreciation for TRL to contribute atherogenesis, we sought to evaluate the effect of nobiletin on intestinal TRL metabolism in both *Ldlr*^{−/−} and WT mice. In the present study, HFHC-feeding in male *Ldlr*^{−/−} mice reduced intestinal insulin sensitivity leading to enhanced intestinal de novo lipogenesis, which, together with dietary lipids, led to greater triglyceride storage resulting in prolonged postprandial lipemia. The addition of nobiletin to the HFHC diet in male *Ldlr*^{−/−} mice improved intestinal insulin sensitivity, attenuated de novo synthesis pathways, promoting efficient dietary triglyceride excursion from the intestine into plasma. Correspondingly, we observed a shortened period of postprandial lipemia with nobiletin treatment compared with *Ldlr*^{−/−} mice fed the HFHC diet alone, which may contribute to nobiletin's protection from atherosclerosis. Many of these results were reproduced in male WT mice but not in female *Ldlr*^{−/−} mice (Table S1).

Studies in humans and hamsters reveal an overproduction of apoB48-containing particles in the context of insulin resistance.^{13,35,46} In HFHC-fed *Ldlr*^{−/−} mice, higher postprandial plasma apoB48 was only observed 4-hours postgavage. Several studies indicate a delayed intestinal-triglyceride secretion rate in diet-induced obese mice,^{10,16} which we now demonstrate is prevented by nobiletin. Despite this nobiletin-enhanced excursion, we did not detect a difference in plasma apoB48 secretion compared with HFHC alone. This data suggested that the same number of particles are secreted and our triglyceride:apoB48 ratio analyses revealed that nobiletin treatment leads to a greater amount of triglyceride per intestinal lipoprotein particle compared with HFHC-fed mice. The VLDL fraction, postgavage, was assumed to be predominantly intestinally derived, by the rapid rise in plasma VLDL-triglyceride following the oil gavage. However, a noted limitation of our study is unlike hamster models, we cannot differentiate the origin of apoB48 as hepatic or enterocyte in mice.¹³ Nevertheless, we have previously shown that nobiletin decreased the fasting VLDL-triglyceride secretion rate to <1 mmol/L per hour,²⁶ representing <20% of the postoil gavage VLDL-triglyceride secretion rate observed in the present study.

In our HFHC-fed WT mice, however, higher plasma apoB48 was observed at 2- and 4-hour postgavage compared with nobiletin-treated mice and SLD controls. Still, nobiletin treatment led to enhanced intestinal-triglyceride secretion, suggesting a possible dysregulation of the LDLR (LDL receptor) with HFHC-feeding that is prevented by

nobiletin. Indeed, basolateral reuptake of chylomicrons via the LDLR has been shown in enterocytes; a process inhibited by apoC-III.⁴⁷ While we did not measure circulating apoC-III, we did observe a significantly higher mRNA expression of jejunal *Apoc3* in HFHC-fed WT mice that was prevented by nobiletin. Whether enhanced postprandial chylomicron secretion contributes to nobiletin's ability to prevent diet-induced obesity or is secondary to weight gain prevention could not be deduced from this study. Moreover, whether HFHC diet-induced changes in intestinal-triglyceride secretion rates correspond to structural changes in the small intestine (longer villi and shorter gut length) requires further investigation, particularly given that nobiletin treatment attenuates these changes.

The peak postprandial triglyceride levels with nobiletin, which occurred 1 hour earlier compared with HFHC-fed mice, were consistent with measures of enhanced triglyceride clearance in nobiletin-treated mice. Enhanced LPL activity has been reported in Western-diet fed *Ldlr*^{−/−} supplemented with the citrus flavonoid naringenin.³⁰ While our study did not directly measure LPL activity, VLDL and chylomicrons compete for LPL-mediated hydrolysis, where the latter is the preferred substrate due to their greater size.⁴⁸ In WT mice, nobiletin treatment enhanced the clearance of injected chylomicrons. Therefore, the delayed, yet prolonged chylomicron secretion exhibited by HFHC-fed mice likely extends the retention of hepatic and intestinal VLDL-sized particles in the circulation. Conversely, the accelerated gastric emptying, efficient intestinal-triglyceride secretion, together with enhanced triglyceride clearance in nobiletin-treated mice suggests improved systemic energy utilization resulting in lower fasting plasma triglyceride.

HFHC-fed mice accumulated jejunal triglyceride in the fed state, which eventually cleared after 9 hours of fasting. We previously reported that nobiletin significantly reduced fasting liver and jejunal triglyceride; importantly, these studies demonstrated that caloric intake and intestinal triglyceride absorption were not affected by nobiletin.²⁶ The present study demonstrated that nobiletin-treated mice do not accumulate jejunal triglyceride more than SLD-fed mice, even in the fed state. Despite the limited jejunal triglyceride storage, nobiletin enhanced *Plin2* mRNA expression in all models tested compared with HFHC-fed mice. *PLIN2* localization to CLD is a response to chronic high-fat feeding,³⁶ and in our study, electron micrographs reveal the presence of smaller CLD in nobiletin-treated mice. Furthermore, the consistently higher expression of *Plin2* by nobiletin in all models tested appears to be independent of changes in postprandial lipid metabolism. Consistent with a previous study,⁴⁹ we showed that HFHC-fed mice have a greater jejunal FA oxidation capacity compared with SLD-fed mice, which remained high with nobiletin treatment. Therefore, in contrast to the liver, enhanced FA oxidation is not the dominant mechanism for triglyceride reduction in the intestine. Instead, LTT experiments in this study revealed that nobiletin limited intestinal lipid stores

by enhancing the rate at which total triglyceride mass (from stored and acute dietary pools) and radiolabeled-triglyceride (traces only dietary triglyceride) were secreted into plasma compared with HFHC-fed mice.

These studies also assessed the potential for HFHC-induced bifurcation in insulin signaling in the intestine of male *Ldlr*^{-/-} mice, a mechanism well-characterized in the liver.¹⁸ The insulin-sensitizing properties of nobiletin were apparent in the jejunum with higher levels of phosphorylated AKT and FOXO1 upon refeeding compared with HFHC- and SLD-fed mice. While the relationship between increased intestinal-triglyceride secretion rate and increased FOXO1 phosphorylation is unclear, these data support a different role for FOXO1 in the intestine compared with the liver.⁵⁰ Downstream of mTORC1, improved insulin sensitivity by nobiletin led to lower jejunal Srebf1c mRNA expression in the refed and post-olive oil states compared with HFHC-fed mice, leading to reduced FA synthesis. Nobiletin also reduced NEFA availability, contributing to smaller intestinal triglyceride stores. Despite higher plasma GLP-1, and presumably GLP-2, in nobiletin-treated mice, signaling through GLP-1R or GLP-2R did not significantly impact intestinal-triglyceride secretion or other aspects of metabolic protection, including prevention of HFHC diet-induced shortening of the small intestine. Collectively, these results suggest that the prevention of diet-induced insulin resistance exerted by nobiletin in the atherogenic model of *Ldlr*^{-/-} male mice played an important role in limiting excess FA and triglyceride substrate for intestinal lipid storage and in promoting accelerated TRL secretion.

In summary, nobiletin prevents diet-induced intestinal lipid accumulation in male mice by normalizing de novo lipogenesis through improved insulin sensitivity and increased postprandial TRL-triglyceride intestinal secretion and plasma triglyceride clearance. Furthermore, the nobiletin-induced enhancement of plasma triglyceride clearance more than compensates for the accelerated TRL-triglyceride secretion, resulting in the prevention of postprandial lipemia which may contribute to the anti-atherogenic effects of nobiletin treatment.

ARTICLE INFORMATION

Received September 25, 2020; accepted November 29, 2021.

Affiliations

Molecular Medicine, Robarts Research Institute (N.M.M., D.E.T., S.S.C., B.G.S., J.Y.E., M.W.H.), Department of Biochemistry (N.M.M., S.S.C., M.W.H.), and Department of Medicine (D.E.T., J.Y.E., M.W.H.), The University of Western Ontario, London, Canada. The University of Ottawa Heart Institute, Ontario, Canada (N.M.M., N.A.T., A.A.H., E.F., E.E.M.). Centre for Infection, Immunity and Inflammation, Ottawa, Ontario, Canada (E.E.M.). Montreal Diabetes Research Group, Montreal, Quebec, Canada (E.E.M.). Department of Biochemistry, Microbiology and Immunology, The University of Ottawa, Faculty of Medicine, ON (N.M.M., N.A.T., A.A.H., E.F., E.E.M.).

Acknowledgments

We thank the UWO Biotron for sample preparation, sectioning, staining and electron microscopy, the Molecular Pathology Core Facility at the University of Western Ontario for assistance with histology. M.W. Huff and E.E. Mulvihill are the guarantors of this work and, as such, had full access to all the data in the study and take respon-

sibility for the integrity of the data and the accuracy of the data analysis. The study concept and design done by N.M. Morrow, M.W. Huff, and E.E. Mulvihill. The acquisition of data was done by N.M. Morrow, D.E. Telford, B.G. Sutherland, J.Y. Edwards, N.A. Trzaskalski, S.S. Chhoker, E. Fadzeyeva, A.A. Hanson, and E.E. Mulvihill. The analysis and interpretation of data was done by N.M. Morrow, D.E. Telford, B.G. Sutherland, J.Y. Edwards, N.A. Trzaskalski, S.S. Chhoker, A.A. Hanson, and E.E. Mulvihill. The drafting of the article was done by N.M. Morrow, M.W. Huff, and E.E. Mulvihill. The critical revision of the article for important intellectual content was done by N.M. Morrow, D.E. Telford, B.G. Sutherland, J.Y. Edwards, N.A. Trzaskalski, A.A. Hanson, E. Fadzeyeva, M.W. Huff, and E.E. Mulvihill. The statistical analysis was done by N.M. Morrow, M.W. Huff, and E.E. Mulvihill. Funding was obtained by M.W. Huff and E.E. Mulvihill.

Sources of Funding

This work was supported by Canadian Institutes of Health Research Grants, ARJ-162628 and Project Grant 156136 to E.E. Mulvihill, MOP-126045 and MOP-119350 to M.W. Huff, NSERC grant 551669-152199-2004 to E.E. Mulvihill and Heart and Stroke Foundation of Canada Grant G-14-0006179 to M.W. Huff. E.E. Mulvihill is the recipient of a Diabetes Canada New Investigator Award.

Disclosures

E.E. Mulvihill receives funding from the Merck IISP program for preclinical studies unrelated to this work. The other authors report no conflicts.

Supplemental Material

Figures S1–S2
Table S1
Expanded Materials & Methods
Major Resources Table

REFERENCES

- Wu L, Parhofer KG. Diabetic dyslipidemia. *Metabolism*. 2014;63:1469–1479. doi: 10.1016/j.metabol.2014.08.010
- Xiao C, Dash S, Morgantini C, Hegele RA, Lewis GF. Pharmacological targeting of the atherogenic dyslipidemia complex: the next frontier in CVD prevention beyond lowering LDL cholesterol. *Diabetes*. 2016;65:1767–1778. doi: 10.2337/db16-0046
- Fan W, Philip S, Granowitz C, Toth PP, Wong ND. Residual hypertriglyceridemia and estimated atherosclerotic cardiovascular disease risk by statin use in U.S. adults with diabetes: National Health and Nutrition Examination Survey 2007–2014. *Diabetes Care*. 2019;42:2307–2314. doi: 10.2337/dc19-0501
- Bhatt DL, Steg PG, Miller M. Cardiovascular risk reduction with icosapent ethyl. *N Engl J Med*. 2019;380:1678. doi: 10.1056/NEJMc1902165
- Iqbal J, Hussain MM. Intestinal lipid absorption. *Am J Physiol Endocrinol Metab*. 2009;296:E1183–E1194. doi: 10.1152/ajpendo.90899.2008
- Mulvihill EE. Regulation of intestinal lipid and lipoprotein metabolism by the proglucagon-derived peptides glucagon like peptide 1 and glucagon like peptide 2. *Curr Opin Lipidol*. 2018;29:95–103. doi: 10.1097/MOL.0000000000000495
- Pavlic M, Xiao C, Szeto L, Patterson BW, Lewis GF. Insulin acutely inhibits intestinal lipoprotein secretion in humans in part by suppressing plasma free fatty acids. *Diabetes*. 2010;59:580–587. doi: 10.2337/db09-1297
- Duez H, Lamarche B, Uffelman KD, Valero R, Cohn JS, Lewis GF. Hyperinsulinemia is associated with increased production rate of intestinal apolipoprotein B-48-containing lipoproteins in humans. *Arterioscler Thromb Vasc Biol*. 2006;26:1357–1363. doi: 10.1161/01.ATV.0000222015.76038.14
- Tran TT, Postal BG, Demignot S, Ribeiro A, Osinski C, Pais de Barros JP, Blachnio-Zabielska A, Leturque A, Rousset M, Ferré P, et al. Short Term Palmitate Supply Impairs Intestinal Insulin Signaling via Ceramide Production. *J Biol Chem*. 2016;291:16328–16338. doi: 10.1074/jbc.M115.709626
- Uchida A, Whitsitt MC, Eustaquio T, Slipchenko MN, Leary JF, Cheng JX, Buhman KK. Reduced triglyceride secretion in response to an acute dietary fat challenge in obese compared to lean mice. *Front Physiol*. 2012;3:26. doi: 10.3389/fphys.2012.00026
- Zoltowska M, Ziv E, Delvin E, Sinnett D, Kalman R, Garofalo C, Seidman E, Levy E. Cellular aspects of intestinal lipoprotein assembly in *Psammomys obesus*: a model of insulin resistance and type 2 diabetes. *Diabetes*. 2003;52:2539–2545. doi: 10.2337/diabetes.52.10.2539
- D'Aquila T, Hung YH, Carreiro A, Buhman KK. Recent discoveries on absorption of dietary fat: presence, synthesis, and metabolism of cytoplasmic lipid droplets within enterocytes. *Biochim Biophys Acta*. 2016;1861(8 Pt A):730–747. doi: 10.1016/j.bbalip.2016.04.012

13. Haidari M, Leung N, Mahbub F, Uffelman KD, Kohen-Avramoglu R, Lewis GF, Adeli K. Fasting and postprandial overproduction of intestinally derived lipoproteins in an animal model of insulin resistance. Evidence that chronic fructose feeding in the hamster is accompanied by enhanced intestinal de novo lipogenesis and ApoB48-containing lipoprotein overproduction. *J Biol Chem*. 2002;277:31646–31655. doi: 10.1074/jbc.M200544200
14. Dalby MJ, Ross AW, Walker AW, Morgan PJ. Dietary uncoupling of gut microbiota and energy harvesting from obesity and glucose tolerance in mice. *Cell Rep*. 2017;21:1521–1533. doi: 10.1016/j.celrep.2017.10.056
15. Zhu J, Lee B, Buhman KK, Cheng JX. A dynamic, cytoplasmic triacylglycerol pool in enterocytes revealed by ex vivo and in vivo coherent anti-Stokes Raman scattering imaging. *J Lipid Res*. 2009;50:1080–1089. doi: 10.1194/jlr.M800555-JLR200
16. Douglass JD, Malik N, Chon SH, Wells K, Zhou YX, Choi AS, Joseph LB, Storch J. Intestinal mucosal triacylglycerol accumulation secondary to decreased lipid secretion in obese and high fat fed mice. *Front Physiol*. 2012;3:25. doi: 10.3389/fphys.2012.00025
17. Saiyo M, Kobayashi T, Masuda D, Kanno K, Zhu Y, Okada T, Koseki M, Ohama T, Nishida M, Sakata Y, et al. A novel selective PPAR α modulator (SPPAR α), K-877 (Pemafibrate), attenuates postprandial hypertriglyceridemia in Mice. *J Atheroscler Thromb*. 2018;25:142–152. doi: 10.5551/jat.39693
18. Brown NM, Goldstein JL. Selective versus total insulin resistance: a pathogenic paradox. *Cell Metab*. 2008;7:95–96. doi: 10.1016/j.cmet.2007.12.009
19. Sears B, Perry M. The role of fatty acids in insulin resistance. *Lipids Health Dis*. 2015;14:121. doi: 10.1186/s12944-015-0123-1
20. Czech MP. Insulin action and resistance in obesity and type 2 diabetes. *Nat Med*. 2017;23:804–814. doi: 10.1038/nm.4350
21. Mulvihill EE, Burke AC, Huff MW. Citrus flavonoids as regulators of lipoprotein metabolism and atherosclerosis. *Annu Rev Nutr*. 2016;36:275–299. doi: 10.1146/annurev-nutr-071715-050718
22. Morrow NM, Burke AC, Samsondar JP, Seigel KE, Wang A, Telford DE, Sutherland BG, O'Dwyer C, Steinberg GR, Fullerton MD, et al. The citrus flavonoid nobiletin confers protection from metabolic dysregulation in high-fat-fed mice independent of AMPK. *J Lipid Res*. 2020;61:387–402. doi: 10.1194/jlr.RA119000542
23. He B, Nohara K, Park N, Park YS, Guillory B, Zhao Z, Garcia JM, Koike N, Lee CC, Takahashi JS, et al. The small molecule nobiletin targets the molecular oscillator to enhance circadian rhythms and protect against metabolic syndrome. *Cell Metab*. 2016;23:610–621. doi: 10.1016/j.cmet.2016.03.007
24. Kim YJ, Choi MS, Woo JT, Jeong MJ, Kim SR, Jung UJ. Long-term dietary supplementation with low-dose nobiletin ameliorates hepatic steatosis, insulin resistance, and inflammation without altering fat mass in diet-induced obesity. *Mol Nutr Food Res*. 2017;61.
25. Lee YS, Cha BY, Choi SS, Choi BK, Yonezawa T, Teruya T, Nagai K, Woo JT. Nobiletin improves obesity and insulin resistance in high-fat diet-induced obese mice. *J Nutr Biochem*. 2013;24:156–162. doi: 10.1016/j.jnutbio.2012.03.014
26. Mulvihill EE, Assini JM, Lee JK, Allister EM, Sutherland BG, Koppes JB, Sawyez CG, Edwards JY, Telford DE, Charbonneau A, et al. Nobiletin attenuates VLDL overproduction, dyslipidemia, and atherosclerosis in mice with diet-induced insulin resistance. *Diabetes*. 2011;60:1446–1457. doi: 10.2337/db10-0589
27. Burke AC, Sutherland BG, Telford DE, Morrow MR, Sawyez CG, Edwards JY, Drangova M, Huff MW. Intervention with citrus flavonoids reverses obesity and improves metabolic syndrome and atherosclerosis in obese Ldlr $^{-/-}$ mice. *J Lipid Res*. 2018;59:1714–1728. doi: 10.1194/jlr.M087387
28. Lee SJ, Lee J, Li KK, Holland D, Maughan H, Guttman DS, Yusta B, Drucker DJ. Disruption of the murine Glp2r impairs Paneth cell function and increases susceptibility to small bowel enteritis. *Endocrinology*. 2012;153:1141–1151. doi: 10.1210/en.2011-1954
29. Assini JM, Mulvihill EE, Sutherland BG, Telford DE, Sawyez CG, Felder SL, Chhoker S, Edwards JY, Gros R, Huff MW. Naringenin prevents cholesterol-induced systemic inflammation, metabolic dysregulation, and atherosclerosis in Ldlr $^{-/-}$ mice. *J Lipid Res*. 2013;54:711–724. doi: 10.1194/jlr.M032631
30. Mulvihill EE, Allister EM, Sutherland BG, Telford DE, Sawyez CG, Edwards JY, Markle JM, Hegele RA, Huff MW. Naringenin prevents dyslipidemia, apolipoprotein B overproduction, and hyperinsulinemia in LDL receptor-null mice with diet-induced insulin resistance. *Diabetes*. 2009;58:2198–2210. doi: 10.2337/db09-0634
31. Shirai N, Geoly FJ, Bobrowski WF, Okerberg C. The application of para-phenylenediamine staining for assessment of phospholipidosis. *Toxicol Pathol*. 2016;44:1160–1165. doi: 10.1177/0192623316673921
32. Hung YH, Carreiro AL, Buhman KK. Dgat1 and Dgat2 regulate enterocyte triacylglycerol distribution and alter proteins associated with cytoplasmic lipid droplets in response to dietary fat. *Biochim Biophys Acta Mol Cell Biol Lipids*. 2017;1862:600–614. doi: 10.1016/j.bbalip.2017.02.014
33. Adomshick V, Pu Y, Veiga-Lopez A. Automated lipid droplet quantification system for phenotypic analysis of adipocytes using CellProfiler. *Toxicol Mech Methods*. 2020;30:378–387. doi: 10.1080/15376516.2020.1747124
34. Ramms B, Gordts PLSM. Apolipoprotein C-III in triglyceride-rich lipoprotein metabolism. *Curr Opin Lipidol*. 2018;29:171–179. doi: 10.1097/MOL.0000000000000502
35. Adeli K, Lewis GF. Intestinal lipoprotein overproduction in insulin-resistant states. *Curr Opin Lipidol*. 2008;19:221–228. doi: 10.1097/MOL.0b013e3282ffaf82
36. Lee B, Zhu J, Wolins NE, Cheng JX, Buhman KK. Differential association of adipophilin and TIP47 proteins with cytoplasmic lipid droplets in mouse enterocytes during dietary fat absorption. *Biochim Biophys Acta*. 2009;1791:1173–1180. doi: 10.1016/j.bbalip.2009.08.002
37. Frank DN, Bales ES, Monks J, Jackman MJ, MacLean PS, Ir D, Robertson CE, Orlicky DJ, McManaman JL. Perilipin-2 modulates lipid absorption and microbiome responses in the mouse intestine. *PLoS One*. 2015;10:e0131944. doi: 10.1371/journal.pone.0131944
38. Drucker DJ, Habener JF, Holst JJ. Discovery, characterization, and clinical development of the glucagon-like peptides. *J Clin Invest*. 2017;127:4217–4227. doi: 10.1172/JCI97233
39. Soares A, Beraldi EJ, Ferreira PE, Bazotte RB, Buttow NC. Intestinal and neuronal myenteric adaptations in the small intestine induced by a high-fat diet in mice. *BMC Gastroenterol*. 2015;15:3. doi: 10.1186/s12876-015-0228-z
40. Tanaka S, Nemoto Y, Takei Y, Morikawa R, Oshima S, Nagaishi T, Okamoto R, Tsuchiya K, Nakamura T, Stutte S, et al. High-fat diet-derived free fatty acids impair the intestinal immune system and increase sensitivity to intestinal epithelial damage. *Biochem Biophys Res Commun*. 2020;522:971–977. doi: 10.1016/j.bbrc.2019.11.158
41. Koehler JA, Baggio LL, Yusta B, Longuet C, Rowland KJ, Cao X, Holland D, Brubaker PL, Drucker DJ. GLP-1R agonists promote normal and neoplastic intestinal growth through mechanisms requiring Fgf7. *Cell Metab*. 2015;21:379–391. doi: 10.1016/j.cmet.2015.02.005
42. Drucker DJ, Yusta B. Physiology and pharmacology of the enteroendocrine hormone glucagon-like peptide-2. *Annu Rev Physiol*. 2014;76:561–583. doi: 10.1146/annurev-physiol-021113-170317
43. Stahel P, Xiao C, Davis X, Tso P, Lewis GF. Glucose and GLP-2 (Glucagon-Like Peptide-2) mobilize intestinal triglyceride by distinct mechanisms. *Arterioscler Thromb Vasc Biol*. 2019;39:1565–1573. doi: 10.1161/ATVBAHA.119.313011
44. Baldassano S, Amato A, Cappello F, Rappa F, Mulè F. Glucagon-like peptide-2 and mouse intestinal adaptation to a high-fat diet. *J Endocrinol*. 2013;217:11–20. doi: 10.1530/JOE-12-0500
45. Baldassano S, Amato A, Rappa F, Cappello F, Mulè F. Influence of endogenous glucagon-like peptide-2 on lipid disorders in mice fed a high-fat diet. *Endocr Res*. 2016;41:317–324. doi: 10.3109/07435800.2016.1141950
46. Federico LM, Naples M, Taylor D, Adeli K. Intestinal insulin resistance and aberrant production of apolipoprotein B48 lipoproteins in an animal model of insulin resistance and metabolic dyslipidemia: evidence for activation of protein tyrosine phosphatase-1B, extracellular signal-related kinase, and sterol regulatory element-binding protein-1c in the fructose-fed hamster intestine. *Diabetes*. 2006;55:1316–1326. doi: 10.2337/db04-1084
47. Li D, Rodia CN, Johnson ZK, Bae M, Muter A, Heussinger AE, Tambini N, Longo AM, Dong H, Lee JY, et al. Intestinal basolateral lipid substrate transport is linked to chylomicron secretion and is regulated by apoC-III. *J Lipid Res*. 2019;60:1503–1515. doi: 10.1194/jlr.M092460
48. Julve J, Martin-Campos JM, Escolà-Gil JC, Blanco-Vaca F. Chylomicrons: advances in biology, pathology, laboratory testing, and therapeutics. *Clin Chim Acta*. 2016;455:134–148. doi: 10.1016/j.ccca.2016.02.004
49. Kondo H, Minegishi Y, Komine Y, Mori T, Matsumoto I, Abe K, Tokimitsu I, Hase T, Murase T. Differential regulation of intestinal lipid metabolism-related genes in obesity-resistant A/J vs. obesity-prone C57BL/6J mice. *Am J Physiol Endocrinol Metab*. 2006;291:E1092–E1099. doi: 10.1152/ajpendo.00583.2005
50. Rajas F, Bruni N, Montano S, Zitoun C, Mithieux G. The glucose-6-phosphatase gene is expressed in human and rat small intestine: regulation of expression in fasted and diabetic rats. *Gastroenterology*. 1999;117:132–139. doi: 10.1016/s0016-5085(99)70559-7